Aus der Klinik für Hals-Nasen-Ohrenheilkunde und

der Klinik für Gynäkologie mit Schwerpunkt gynäkologische Onkologie

der Medizinischen Fakultät Charité-Universitätsmedizin Berlin

DISSERTATION

Disulfiram (Antabuse) acts as a potent chemo-radio sensitizer and abolishes stem cells in HNSCC cell lines *in vitro*

zur Erlangung des akademischen Grades

Doctor medicinae (Dr. med.)

vorgelegt der Medizinischen Fakultät

Charité – Universitätsmedizin Berlin

von

Wenhao Yao

aus Liao Ning, China

Datum der Promotion:

21.06.2020

CONTENTS

Contents i

Abbreviations v

Summary 1

Zusammenfassung 2

1. Introduction 4

1.1 Head and neck squamous cell carcinoma (HNSCC) treatment 4

1.2 Cancer stem cells (CSCs) and stemness-related markers 5

1.3 Aldehyde dehydrogenase (ALDH) is a CSC marker and target for potential treatment . 6

1.4 Anti-cancer effect of DSF or DSF/Cu^{2+} 7

2. Aim of study 8

3. Materials 9

3.1 Laboratory equipment 9

3.2 Chemicals and reagents 10

3.3 Human HNSCC cell lines 10

3.4 Cell culture medium 10

3.5 Kits and other materials 11

4. Methods 12

4.1 Cell culture 12

4.2 Drug preparation 12

4.3 Spheroid formation assay 12

4.4 MTT cytotoxicity assay and CI-isobologram analysis 13

4.5 Flow cytometric analysis for cellular apoptosis 13

4.6 Flow cytometric analysis for Caspase-3 activity 14

4.7 Flow cytometric analysis for cell cycle 14

4.8 Flow cytometric analysis for ROS activity 14

4.9 Irradiation (IR) 14

4.10 Clonogenic assay 15

4.11 Flow cytometric analysis for ALDH activity and cell sorting 15

4.12 Quantitative Real-time Polymerase Chain Reaction (qRT-PCR) 16

4.13 Wound healing assay 16

4.14 Statistical analysis 17

5. Results 18

5.1 ALDH expression is higher in spheroid-derived cells (SDCs) versus monolayer-derived cells (MDCs) in HNSCC cell lines 18

5.2 Stemness-related TFs over-expression in SDCs 18

5.3 DSF exhibits dose- and time-dependent cytotoxicity in HNSCC cell lines 20

5.4 DSF/Cu^{2+} significantly increases cytotoxicity of HNSCC cell lines in a dose- and time-dependent manner 20

5.5 DSF or DSF/Cu^{2+} induces apoptosis in HNSCC cell lines 23

5.6 No significant cell cycle distribution effect by DSF or DSF/Cu^{2+} in HNSCC cell lines 25

5.7 DSF or DSF/Cu^{2+} triggers ROS generation in HNSCC cell lines 26

5.8 DSF or DSF/Cu^{2+} inhibits ALDH enzyme activity in SDCs 28

5.9 DSF or DSF/Cu^{2+} inhibits the expression of stemness-related TFs in SDCs 28

5.10 Inhibition of colony formation by DSF or DSF/Cu^{2+} in HNSCC cell lines 30

5.11 Inhibition of spheroid formation by DSF or DSF/Cu^{2+} in HNSCC cell lines 30

5.12 Inhibition of migratory ability by DSF or DSF/Cu^{2+} in HNSCC cell lines 31

5.13 Increase of colony formation, spheroid formation, and decrease of ROS activity in ALDH ^{high} cells versus ALDH ^{low} cells 34

5.14 DSF overcomes the resistance of cisplatin in ALDH ^{high} cells 34

5.15 DSF and cisplatin combination induce synergistically cytotoxicity 36

5.16 DSF or DSF/Cu^{2+} abolishes cisplatin-induced G2/M phase arrest 36

5.17 Radio-sensitizing effect of DSF or DSF/Cu^{2+} 39

5.18 Combination of DSF or DSF/Cu^{2+} attenuate IR-induced G2/M phase arrest 39

5.19 Analysis of cytotoxicity by triple treatment with DSF or DSF/Cu^{2+}, cisplatin, and IR in HNSCC cell lines 43

5.20 Treatment with DSF or DSF/Cu^{2+}, cisplatin, and IR induce ROS generation in HNSCC cell lines 45

6. Discussion 47

7. References 52

8. Curriculum Vitae 58

9. Affidavit 59

10. Acknowledgements 60

List of Figures

Figure 1: Expression of ALDH and stemness-related TFs in MDCs and SDCs..... 19

Figure 2: Cytotoxicity of DSF or DSF/Cu^{2+} in HNSCC cell lines..... 21

Figure 3: DSF or DSF/Cu^{2+} induces apoptosis in HNSCC cell lines..... 23

Figure 4: No significant cell cycle distribution effect by DSF or DSF/Cu^{2+} in HNSCC cell lines..... 25

Figure 5: DSF or DSF/Cu^{2+} triggers ROS generation in HNSCC cell lines..... 26

Figure 6: DSF or DSF/Cu^{2+} inhibits ALDH expression and stemness-related TFs expression of SDCs in HNSCC cell lines..... 29

Figure 7: DSF or DSF/Cu^{2+} inhibits colony formation, spheroid formation and migratory ability in HNSCC cell lines..... 32

Figure 8: Analysis of stemness, ROS activity, and cisplatin sensitivity in ALDH-sorted cells35

Figure 9: Combination with DSF or DSF/Cu^{2+} and cisplatin in HNSCC cell lines..... 38

Figure 10: Radiosensitizing effect of DSF or DSF/Cu^{2+} in HNSCC cell lines..... 41

Figure 11: DSF or DSF/Cu^{2+} combined with cisplatin and IR enhance apoptosis in HNSCC cell lines..... 43

Figure 12: DSF or DSF/Cu^{2+} combined with cisplatin and IR induce ROS generation in HNSCC cell lines..... 45

List of Tables

Table 1: Combination treatment with DSF and cisplatin results in synergistic cytotoxic effect in HNSCC cell lines..... 37

Abbreviations

ALDH	Aldehyde Dehydrogenase
bFGF	Basic Fibroblast Growth Factor
DMSO	Dimethylsulfoxide
DNA	Deoxyribonucleic Acid
EGF	Epidermal Growth Factor
EDTA	Ethylenediaminetetraacetic Acid
FACS	Fluorescence Activated Cell Sorter
FBS	Fetal Bovine Serum
MDCs	Monolayer-derived Cells
MTT	1-(4,5-Dimethythiazol-2-yl)-3,5-diphenylformazan
Oct3/4	Octamer-binding Transcription Factor 3/4
PBS	Phosphate-buffered Saline
PI	Propidium Iodide
ROS	Reactive Oxygen Species
RNA	Ribonucleic Acid
SDCs	Spheroid-derived Cells
Sox2	Sex-determined Region Y-box 2

Summary

Background: The unfavorable prognosis for locally advanced and metastatic head and neck squamous cell carcinoma (HNSCC) is primarily due to the resistance of cancer stem cells (CSCs) to radio-chemotherapy. ALDH (Aldehyde Dehydrogenase) has been used as a marker to identify CSCs in several tumors including HNSCC. Disulfiram (DSF) is a pan-ALDH inhibitor, which has been found to have remarkable anti-cancer activity. Moreover, DSF is a strong bivalent metal ion chelator, which binds copper (Cu^{2+}) and is responsible for enhanced cytotoxicity.

Methods: Cell viability was assessed using proliferation and apoptosis assays. A synergistic effect was defined by calculating the combination index (CI). ALDH activity was determined by ALDELUOR assay. Stemness-related transcription factors (TFs) were detected by qRT-PCR (Quantitative Real-time Polymerase Chain Reaction), and cellular self-renewal was measured by sphere- and colony-formation. Migration ability was performed by wound healing assay. Cell cycle and Reactive Oxygen Species (ROS) activity were analyzed by flow cytometry.

Results: Our results showed a strong anti-proliferative effect of DSF in a dose- and time-dependent manner, and Cu^{2+} addition dramatically enhanced cytotoxicity. DSF or DSF/Cu^{2+} significantly reduced the proportion of ALDH ^{high} CSCs (e.g. from 59.8% to 33% and 30.0% in UM-SCC9) and stemness-related TFs. They reduced colony formation (e.g. from 145 to 72 and 70 in UM-SCC9), spheroid formation (e.g. from 39 to 18 and 20 in UM-SCC9), and migration ability (e.g. from 71.85% to 42.1% and 43.49% in UM-SCC9). DSF or DSF/Cu^{2+} induced ROS generation and triggered cellular apoptosis. DSF or DSF/Cu^{2+} abolished the cisplatin-induced cell cycle G2/M phase arrest (e.g. from 52.9% to 41.2% and 42.2% in UM-SCC9), overcame the resistance of cisplatin in ALDH ^{high} cells, and showed a synergistic effect in combination with cisplatin (CI<1). Combining radiation (IR) with DSF or DSF/Cu^{2+} showed a growth inhibition and attenuated the cell cycle G2/M phase arrest (e.g. from 53.6% to 40.2% and 41.9% in UM-SCC9). Moreover, the triple treatment with DSF or DSF/Cu^{2+}, cisplatin, and IR enhanced radio-chemo sensitivity by inducing apoptosis (e.g. 42.04% and 32.21% in UM-SCC9) and ROS activity (e.g. 46.3% and 37.4% in UM-SCC9).

Conclusions: Our data demonstrate that DSF or DSF/Cu^{2+} inhibits CSC properties by blocking ALDH enzymatic function. Furthermore, DSF or DSF/Cu^{2+} in combination with cisplatin and IR enhance cytotoxicity and induce ROS activity. Thus, our findings hold promise for pre- and further clinical evaluation by repurposing DSF as a radio-chemo sensitizer.

Zusammenfassung

Hintergrund: Die ungünstige Prognose des lokal fortgeschrittenen und metastasierten Plattenepithelkarzinoms im Kopf-Halsbereich (HNSCC) ist vor allem auf die Resistenz von Krebsstammzellen (CSCs) gegen die Radiochemotherapie zurückzuführen. ALDH (Aldehyde Dehydrogenase) wurde als Marker verwendet, um CSCs unterschiedlichen Tumoren, einschließlich HNSCC, zu identifizieren. Disulfiram (DSF) ist ein pan-ALDH-Hemmer, der eine bemerkenswerte Aktivität gegen viele Arten von Krebsarten aufweist. Darüber hinaus ist DSF ein starker bivalenter Metallionen-Chelator, der Kupfer (Cu^{2+}) bindet und für eine erhöhte Zytotoxizität verantwortlich ist.

Methoden: Die Zellvitalität wurde mit Hilfe von Proliferation - und Apoptose-Assays bewertet. Ein synergistischer Effekt wurde durch die Berechnung des Kombinationsindex (CI) definiert. Die ALDH-Aktivität wurde mittels ALDELUOR-Assay und FACS-Sortierung bestimmt. Stemness-related transcription factors (TFs) wurden mittels qRT-PCR (Quantitative Real-time Polymerase Chain Reaction) nachgewiesen und die zelluläre Selbsterneuerung mittels Spheroid- und Koloniebildungstests gemessen. Die Migrationsfähigkeit wurde durch einen Wundheilungstest bestimmt. Zellzyklus und Aktivität der Reaktiven Sauerstoffspezies (ROS) wurden mittels Durchflusszytometrie analysiert.

Ergebnisse: Unsere Ergebnisse zeigten eine starke antiproliferative Wirkung von DSF in dosis- und zeitabhängiger Weise. Hunzufügen von Cu^{2+} führte zu einer drastisch erhöhten Zytotoxizität. DSF oder DSF/Cu^{2+} reduzierten den Anteil an ALDH-Hoch-CSCs (z.B. von 59,8% auf 33,0% und 30,0% in UM-SCC9) und stemnessbezogenen TFs deutlich. Sie reduzierten auch die Koloniebildung (z.B. von 145 auf 72 und 70 in UM-SCC9), die Sphäroidbildung (z.B. von 39 auf 18 und 20 in UM-SCC9) und die Migrationsfähigkeit (z.B. von 71,85% auf 42,1% und 43,49% in UM-SCC9). DSF oder DSF/Cu^{2+} induzierten ROS-Bildung und lösten Apoptose aus. DSF oder DSF/Cu^{2+} haben den Cisplatin-induzierten Zellzyklus G2/M-Phasenstopp (z.B. von 52,9% auf 41,2% und 42,2% bei UM-SCC9) gestoppt, die Resistenz von Cisplatin in ALDH-Hochzellen überwunden und einen synergistischen Effekt in Kombination mit Cisplatin (CI<1) gezeigt. Die Kombination von Strahlung (IR) mit DSF oder DSF/Cu^{2+} zeigte eine signifikante Wachstumshemmung und reduzierte den Zellzyklus G2/M-Phasenstopp (z.B. von 53,6% auf 40,2% und 41,9% bei UM-SCC9). Darüber hinaus resultierte die Dreifachbehandlung mit DSF oder DSF/Cu^{2+}, Cisplatin und IR in einer erhöhte Radiochemosensitivität durch Induktion von Apoptose (z.B. 42,04% und 32,21% in UM-SCC9) und ROS-Aktivität (z.B. 46,3% und 37,4% in

UM-SCC9).

Schlussfolgerung: Unsere Daten zeigen, dass DSF oder DSF/Cu^{2+} die CSCs-Eigenschaften hemmen, indem sie die enzymatische ALDH-Funktion blockieren. Darüber hinaus erhöhten DSF oder DSF/Cu^{2+} in Kombination mit Cisplatin und IR die Zytotoxizität und induzierten ROS-Aktivität. Daher ermutigen unsere Ergebnisse DSF als Radio-Chemosensitizer in präklinischen und klinischen Studien zu bewerten.

1. Introduction

1.1 Head and neck squamous cell carcinoma (HNSCC) treatment

Head and neck cancer is the sixth-most common cancer, accounting for over 550,000 new cases and 380,000 deaths worldwide per year [1], which can arise in the oral cavity, pharynx, larynx, nasal cavity, paranasal sinuses, thyroid, and salivary glands, and include a variety of histopathologic tumors. Among these pathological types, head and neck squamous cell cancer (HNSCC) is the most common one [2]. Despite HNSCC being highly curable at early stages, about 60% of HNSCC patients are diagnosed with loco-regionally advanced disease (stage III–IV), which is still associated with poor curative prognoses, therefore, definitive local therapies, such as surgery, followed by radiation therapy (RT), with or without concomitant chemotherapy (CT), are the key components in the initial treatment of locally advanced (LA) HNSCC [3]. Although general treatment protocols and new advances are being optimized and intensified in the therapy of LA HNSCC, survival rates have remained largely unchanged over the past 30 years, with a five-year overall survival rate of less than 50%, and treatment resistance as well as tumor recurrence remain the critical problems [4]. Thus, there is an urgent need for identification and development of novel therapeutic strategies, which are more effective and have fewer side effects than the currently used treatment regimens.

The organ preservation protocol with chemo-radiation has been developed during recent years and is also increasingly being applied to LA HNSCC, whereby cisplatin-based chemotherapy is combined with concurrent loco-regional radiotherapy [5]. Cisplatin is a potent inducer of apoptosis in several cell types, and is also one of the most effective and widely used chemotherapeutic drugs for the treatment of human cancers, including HNSCC, especially at the advanced stage [6]. Biologically, cisplatin binds to DNA, forming adducts, and also favors the accumulation of intracellular free radicals [7]. Even though it has long history of successful use, cisplatin therapy has two major limitations — severe toxicity and acquired resistance [8]. Consequently, acquiring a better understanding of the molecular basis of cisplatin resistance is warranted in order to elucidate the underlying mechanisms of this drug resistant phenotype, which is the current primary obstacle to the clinical utility of this drug and improving the clinic outcome [9].

RT, either alone or in combination with concurrent systemic chemotherapy as appropriate, remains the mainstay standard of treatment in the curative-intent management of LA and

metastatic HNSCC, both in the definitive non-surgical and post-operative adjuvant settings [10, 11]. Several types of DNA lesion are induced by IR, including changes in the bases of nucleic acids, single-strand breaks, double-strand breaks, and abnormal cross-links in DNA or between DNA and cellular proteins [12]. In response to DNA damage, proliferating cells arrest at specific checkpoints along the cell cycle, by activating a network of signaling pathways. Such pauses allow time for DNA repair and prevent the damaged DNA being replicated and transmitted to the next generation, either by reparation or by induction of cell death. The successful repair of DNA lesions is essential for clonogenic survival and the restoration of genome integrity. If not totally repaired, such lesions might be lethal for the cell, or may impair the integrity of genomic DNA. On the other hand, excessive and persistent DNA damage leads to premature senescence, apoptosis, necrosis or mitotic catastrophe [13-15]. In practice, one of the major challenges in RT is the prediction of the patients' tumor radio-resistance in response to IR, in order to optimize the given dose for maximal tumor cell killing effect, and minimal normal tissue damage [16]. An adaptive response sometimes appears in cancer cells during the treatment process, and tumors showing an adaptive response tend to be more resistant, aggressive, and invasive [17]. Therefore, identifying the underlying mechanisms of radioresistance should a promising strategy to personalize therapy where necessary, thereby achieving better treatment success rates [18].

1.2 Cancer stem cells (CSCs) and stemness-related markers

Cancer stem cells (CSCs) or cancer stem-like cells are a small population in the majority of tumor cells, which are responsible for tumor development, dissemination and recurrence [19]. They display high tumorigenicity and might associate with chemo-radio-therapy resistance in HNSCC. Although CSCs constitute a small minority of neoplastic cells, they are still believed to possess pluripotent and self-renewal capacity, thereby generating a heterogeneous cell population of the originating tumor, seeding at distant sites and driving the formation of macro metastasis [20]. Consequently, it is urgent to identify and develop unique agents to target CSCs, with potentially allows for increased specificity and efficiency in the clinic therapy, thereby enhancing patient survival.

Based on the observations that CSCs contribute to cancer tumorigenicity, it has been suggested that the expression level of stemness genes, or core related factors to CSCs, may be associated with tumor progression. Recently, *in vitro* and *in vivo* research has also highlighted a number of stem-cell surface markers including CD44 and CD133, which could be isolated and measured by flow cytometry, and attribute tumorigenic properties to these CSCs, correlating with recurrence

and diagnosis in HNSCC [21]. Among these genes, the stemness-related TFs Oct3/4, Sox2, and Nanog form primary regulatory networks that coordinate to determine the self-renewal and differentiation of embryonic CSCs [22]. Studies demonstrate that Oct3/4 is highly expressed in human bladder cancer, and is associated with disease progression, increased metastasis, and lower survival [23]. Moreover, Nanog is over-expressed in numbers of cancer types, such as breast, lung, pancreas and ovary [24-27].

Even though the survival of cells with CSC-specific properties in some carcinomas has been attributed to an enhanced ability for drug removal, decreased DNA damage, or increased DNA repair, the mechanisms behind their differential resistance to apoptosis are not yet completely clear, nor have they been investigated in a broad range of carcinomas or in normal human epithelium [28]. Therefore, it is crucial to get more information for their general applicability, especially in HNSCC, which is characterized by particularly high recurrence rates.

1.3 Aldehyde dehydrogenase (ALDH) is a CSC marker and target for potential treatment

The ALDH (Aldehyde dehydrogenase) family is a group of cytosolic isoenzymes that catalyze the oxidation of aldehydes and retinol in cells, and play significant roles in the cellular detoxification and controlling metabolism of retinoic acid (RA), primary for normal growth, differentiation, and development of adult organs and tissues in vertebrates [29]. Bertland et al. found that HNSCC with increased ALDH activity were more resistant to RT, and that the inhibition of ALDH activity increased sensitivity to IR [30]. Prince et al. also suggested that ALDH is a more specific marker for the CSC population than CD44 in HNSCC, which indicates that ALDH ^{high} cells comprise a cell subpopulation that are tumorigenic and capable of initiating tumors at very low numbers, and that ALDH on its own is a highly selective marker for CSCs [31].

ALDH1A1, a core member of ALDH family, is a CSC cell-associated protein in various malignant cancers and its level correlates with the patient's outcome [32]. Recently, ALDH1A1 was found to be increased in tumor spheres [33], and in three-dimensional cultured cancer stem-like cells [34] in esophageal squamous cell carcinoma cells, suggesting that ALDH1A1 might be a more reliable marker for the identification and isolation of CSCs. Furthermore, consistent with our findings, compared with other isoforms (ALDH1A3 and ALDH3A1), over-expression of ALDH1A1 enhanced lung cancer cell transformation. Additioinally, up-regulated expression of

ALDH1A1 is positively associated with the stage and grade of the lung cancer patients, and related to a poor prognosis [35].

1.4 Anti-cancer effect of DSF or DSF/Cu^{2+}

Disulfiram (tetraethylthiuram disulfiram, DSF), a member of dithiocarbamate family with a 297 Da molecular weight, is an ALDH inhibitor that was used as a vermicide in the 1930s and for alcoholism in the 1940s [36, 37]. Accumulating evidence indicates that this existing drug has promising applications, exhibiting potent anti-cancer properties by enhancing conventional anticancer drug-induced apoptosis, decreasing angiogenesis, attenuating tumor growth, and reversing drug-resistance [20, 38]. In the last few years, several both *in vitro* and *in vivo* studies have demonstrated that DSF is highly effective against a number of cancer types such as breast [39], glioblastoma [40], prostate [41], colorectal [38], and melanoma [42]. Furthermore, DSF also enhances the cytotoxicity of several anticancer drugs as well as RT, suggesting it as a potential chemo-radio-therapeutic agent [43]. Additionally, inhibition of ALDH activity has been demonstrated as a potential strategy to suppress CSCs, and the findings indicate that DSF may specifically target CSC subpopulations [44, 45].

As a strong bivalent metal ion chelator, DSF converts to diethyldithiocarbamate (deDTC), and two molecules of deDTC bind to one molecule of copper (Cu^{2+}) to form a complex Cu $(deDTC)_2$ (DSF/Cu) which improves the intracellular trafficking of copper and may probably responsible for DSF-induced apoptosis [46, 47]. Regarding the overall stoichiometry of reaction with respect to Cu^{2+}, the DSF molar ratio is 0.9:1.0, which presumably could be a reference for ratio when DSF acts as a copper ionophore in the substance combination. It is likely that this may be the mechanism for the reaction of DSF with copper (II) ions under biological conditions [48]. Copper is indispensable in life processes, acting with an important effect in inflammation, tumor growth, and stimulating the proliferation and migration of endothelial cells at high concentrations [49, 50]. Moreover, Cu is an important trace element for life as it plays a core role in redox reactions, and triggers generation of reactive oxygen species (ROS) in human cells [47]. In comparison with their normal counterpart, head and neck tumor tissues contain higher levels of Cu [51]. Since basal Cu and intrinsic ROS levels are higher in the tumor cells, the use of DSF represents a potentially new approach to selectively target the cancer cells, limiting the cytotoxic effect associated with Cu overload against normal cells [52]. Consequently, the cytotoxicity of DSF/Cu^{2+} leads to the generation of oxidative stress, inhibition of DNA replication, or modulation of the activity of other critical cellular regulatory pathways [53].

2. Aim of the study

The objective of this thesis was to investigate the cytotoxicity of DSF or DSF/Cu^{2+} in HNSCC, their inhibitory effect on CSCs, and the promising mechanism involving the combination of chemotherapeutic agents (cisplatin) and IR *in vitro*. Therefore, the following aims were pursued:

1. To explore the cytotoxic effect in HNSCC.
2. To compare the expression of ALDH and stemness-related TFs (Oct3/4, Sox2, and Nanog) between monolayer-derived cells and their corresponding spheroid-derived cells.
3. To characterize the inhibitory effect of DSF or DSF/Cu^{2+} on self-renewal capacity and CSC properties in HNSCC cell lines.
4. To assess the combination effect of DSF or DSF/Cu^{2+}, cisplatin, and IR in HNSCC cell lines and the potential mechanism for this combination through cell cycle distribution, cytotoxicity and ROS generation *in vitro*.

3. Materials

3.1 Laboratory Equipment

Freezer (-80 ℃, -150 ℃)	Sanyo, Japan
Axiovert 40C Microscope	Carl ZEISS, Jena, Germany
BD FACS Calibur System	BD Biosciences, Germany
Incubator	Heraeus, Thermo Fisher Scientific, Germany
Centrifuge	Heraeus, Thermo Fisher Scientific, Germany
Pipettes	Eppendorf, Hamburg, Germany
Thermocycler	Julabo, Germany
Vortex-genie 2	Scientific Industries, N.Y., USA

3.2 Chemicals and Reagents

Universal Agarose	Bio&SELL, GmbH, Nuremberg, Germany
Dimethyl Sulfoxide (DMSO)	Sigma-Aldrich, Steinheim, Germany
70% Ethanol	Carl Roth, GmbH, Germany
Epidermal Growth Factor (EGF)	Biochrom GmbH, Berlin, Germany
Fetal Bovine Serum (FBS)	Biochrom AG, Berlin, Germany
Fibroblast Growth Factor-basic (bFGF)	Biochrom GmbH, Berlin, Germany
Penicillin/Streptomycin	Biochrom GmbH, Berlin, Germany
Phosphate Buffered Saline (PBS)	Biochrom GmbH, Berlin, Germany
Trypsin/EDTA	Biochrom GmbH, Berlin, Germany
Chloroform	Merck KGaA, Darmstadt, Germany
Isopropanol	Biochrom GmbH, Berlin, Germany
Trizol Reagent	Ambion, Life Technologies, USA

3.3 Human HNSCC Cell lines

UM-SCC9, UM-SCC47, UMSCC11B: University of Michigan, MI, USA

UT-SCC33: University of Turku, Finland

3.4 Cell Culture Medium

RPMI Medium 1640+GlutaMAX	Gibco, UK

Quantum 263	PAA Laboratories GmbH, Germany

3.5 Kits and Other Material

ALDEFLUOR Assay Kit	Stemcell Technologies, Vancouver, Canada
Annexin-V-FLUOS Staining Kit	Roche, Mannheim, Germany
Power SYBR Green Master Mix	Thermo Fisher Scientific, MA, USA
RevertAid First Strand cDNA Synthesis Kit	Thermo Fisher Scientific, MA, USA
Cell Proliferation Kit I (MTT)	Roche, Mannheim, Germany
MitoSOX Red Mitochondrial Superoxide Indicator	Molecular Probes, Oregon, USA
Caspase-3 Apoptosis Kit,	BD Bioscience, USA
Cellstar Cell Culture Flasks	Greiner Bio-One, Austria
Corning Falcon Tissue Culture Dish	Corning, NY, USA
Falcon Polyptopylene Conical Tubes	Corning, NY, USA
Costar Cell Culture Plates (6-, 12-, 24, 96-well)	Corning, NY, USA
Costar Ultra-low Attachment Cell Culture Plate (24-, 96-well)	Corning, NY, USA
Falcon Cell Strainer (40 μM)	Corning, NY, USA

4. Methods

4.1 Cell Culture

Four HNSCC cell lines UM-SCC9, UM-SCC47, UMSCC11B, and UT-SCC33 were cultured in RPMI 1640 medium supplemented with 10% FBS (heat-inactivated at 56 ℃ for 30 min) and 1% penicillin/streptomycin. Cells were maintained in a 37 ℃ humidified incubator with 95% air and 5% CO_2. All cell experiments were performed in culture for experiments at 70-80% confluence. To harvest and passage them, cells were washed with PBS twice and detached with 0.5%/0.02% Trypsin/EDTA solution. Complete culture medium was added to stop the reaction. After centrifugation at 200*g for 5 min, cells were resuspended into new culture medium for future experiments.

4.2 Drug preparation

Free DSF and copper were dissolved in DMSO and distilled water, respectively, at a stock concentration of 10 mM, and stored at -20 ℃. Cisplatin was kept at a 3.3 mM concentration at room temperature. All drugs were freshly diluted into working concentrations with culture medium before use. A 1:1 ratio of DSF and Cu^{2+} was chosen for all the experiments.

4.3 Spheroid formation assay

First of all, the ultra-low attachment flasks were prepared. 8-10 ml of 1.5% agarose (dissolved in PBS) was filled into cell culture flasks. Then the monolayer cells were cultured in serum-free Quantum 263 supplemented with 10 ng/ml EGF and 10 ng/ml bFGF. 12-15 ml of the cell suspension was added into the cell plates and half of the new culture medium was supplied every 2-3 days. For the passage, the culture medium was removed and the spheroids were harvested into a 40 μM cell strainer, followed by washing twice with PBS. The spheroids were dissociated into single cells using 0.5%/0.02% Trypsin/EDTA in 37 ℃ water bath. After 5-10 min, complete culture medium was added to stop the reaction. All cells were filtered through the 40 μM cell strainer again and reseeded into fresh culture medium under the same conditions for the subsequent experiments.

For the spheroid formation inhibition assay, cells were exposed to DSF or DSF/Cu^{2+} in a 24-well ultra-low attachment plate at a density of $2*10^4$ cells/ml for 3 days. Spheroids of 300 μM or more in diameter were calculated and photographed at 50-fold magnification.

4.4 MTT cytotoxicity assay and CI-isobologram analysis

Assessment of the cytotoxic effect of DSF, DSF/Cu^{2+} or a combination with cisplatin or IR was performed, following 24-72 h of incubation at different drug concentrations, in all tested HNSCC cell lines. Single cells were seeded in triplicate into a 96-well plate at a density of 4000 cells/well in the 100 μl culture medium. Cells without any drug treatments were considered as controls. After the various treatment periods, 10 μl of MTT labeling reagent was added, including to controls, followed by incubation in a 37℃ humidified atmosphere incubator with 95% air and 5% CO_2 for 4 h. When the precipitate was clearly observed at the bottom of the plates, 100 μl of solubilization solution was added to all wells, mixed gently, and was finally incubated overnight. The solution absorbance was quantified at a wavelength of 595 nm using a Bio-Rad microplate reader.

Cellular viability (%) was averaged and normalized against the untreated controls. Dose response curves and IC_{50} values were evaluated using GraphPad Prism 5.0 Software. The cytotoxic relationship between DSF and cisplatin was measured by Chou-Talalay method for drug combination, which is based on the median-effect equation. It provides the theoretical basis for the combination index (CI)-isobologram equation that allows quantitative determination of drug interactions, where CI<1, =1, >1 indicates synergism, additive effect, and antagonism, respectively. CompuSyn software was used for calculation at all doses or effect levels that were simulated automatically [54].

4.5 Flow cytometric analysis for cellular apoptosis

Cells were exposed to different treatments at a density of $3*10^4$/ml for various time intervals in a 24-well plate. The apoptotic effect was measured using the Annexin-V-FLUOS staining kit according to the manufacturer's guidelines. Cells were collected and resuspended in 100 μl labeling solution which contained 20 μl Annexin-V and 20 μl PI at a density of $1*10^7$ cells/ml. Subsequently, cells were incubated at room temperature for 15 min in the dark.

Cellular apoptosis and necrosis were determined using FL3 (PI) and FL1 (Annexin-V) by flow cytometry and measured using FlowJo V10 software. All the cells were divided into 4 quadrants: live cells, lower left (Annexin-V^-/PI^-); early apoptosis, lower right (Annexin-V^+/PI^-); late apoptosis, upper right (Annexin-V^+/PI^+); and necrotic cells, upper left (Annexin-V^-/PI^+).

4.6 Flow cytometric analysis for Caspase-3 activity

Cells were exposed to different concentrations of DSF or DSF/Cu^{2+} at a density of $3*10^4$/ml in a 24-well plate. After 48 h, the apoptosis effect was defined by assessing Caspase-3 activity based on the manufacturer's protocols. In brief, cells were incubated in BD Cytofix/Cytoperm™ solution for 20 min on ice. After washing twice, resuspend cells were labeled with specific antibody for 30 min at room temperature and were then analyzed by flow cytometry.

4.7 Flow cytotmetric analysis for cell cycle

Cells were treated with different concentrations of DSF, DSF/Cu^{2+}, cisplatin, IR, or a combination at a density of $3*10^4$/ml in a 24-well plate for 48 h. Cells without any drug were used as controls. After the incubation time, cells were collected and washed with PBS twice and fixed in 70% cold ethanol at 4℃ overnight. After washing with PBS again, cells were stained with 1 mg/ml PI, 10 mg/ml RNase, and 1% Triton at room temperature for 30 min in the dark. Specifically, in order to avoid cell lose after ethanol fixation, discarding the supernatant was done especially carefully and centrifuging was increased to 3000 rpm for 5 min.

Flow cytometry was used to define the DNA content for all the samples. FlowJo software was used to analyze the percentage of cell cycle distribution in the G0/G1, S, and G2/M phases.

4.8 Flow cytometric analysis for ROS activity

After exposing to various drug treatments for 24 h, the cells were collected and incubated with MitoSOX Red reagent following the manufacturer's instructions in a 37℃ humidified incubator with 95% air and 5% CO_2 for 15 min. Fluorescently labeled ALDH ^{high} and ALDH ^{low} samples, after cell sorting from Aldefluor stained populations, were immediately stained with MitoSOX Red reagent as described above.

After the incubation time and washing with PBS twice, the mean fluorescence intensity was measured by flow cytometry. Cells without any drugs, but incubated with MitoSOX Red reagent, were used as controls.

4.9 Irradiation (IR)

Cells were pre-treated for 4-5 h with different exposures. Subsequently, IR was established with various dosages of 2, 4, 6, or 10 Gy using a medical linear accelerator with a 6 MV photon beam (2.76 Gy/min, Clinac 600 C/D, Varian, Palo Alto, CA, USA). All the cells, maintained in the cell culture plates, were positioned on a plastic foundation for backscatter saturation of the beam to

the plates. An 8 cm-thick solid block of a water-equivalent material was put on the top of the plates to ensure the photon dose exposure to the cells was homogenous. After 24 h, colony formation and ROS activity were determined, and 48 h later, the cell cycle distribution and apoptosis effect were analyzed.

4.10 Clonogenic assay

In the colony formation inhibition assay, cells were treated with DSF or DSF/Cu^{2+} for 24 h at a density of $3*10^4$/ml in 24-well plates. In the IR survival experiments, different treatments of cells were incubated in a 37℃ humidified incubator with 95% air and 5% CO_2 for an additional 24 h after IR. Then, cells were harvested and washed twice with PBS to make sure all the added drugs were completely removed. Single cells were reseeded in the fresh culture medium in 6-well plates. Cells without any treatment were included as controls. After 9-12 days, the medium was removed and colonies were washed with PBS twice before fixation by methanol and staining with 0.5% crystal violet.

A cell population was defined as a colony by consisting of at least 50 cells. Plating efficiency (PE) was assessed as the number of colonies counted/ number of control cells planted. The survival fraction (SF) was the number of colonies observed, divided by the number of cells seeded, with a correction for the PE. The survival curves were determined using the linear-quadratic-model (LQ-Model) and were calculated in the formula Y=exp(-(a*x+b*(x^2))) using GraphPad Prism software.

4.11 Flow cytometric analysis for ALDH activity and cell sorting

Assessment of ALDH enzymatic activity was performed by measuring the ALDH-mediated intracellular reaction of fluorescent compound ALDH substrate BODIPY-aminoacetaldehyde (BAAA), using the Aldefluor assay following the manufacturer's protocols. In brief, all cells were harvest and resuspended in the buffer containing BAAA (1 μmol/L) at a density of $1*10^6$ cells in a 37℃ humidified incubator with 95% air and 5% CO_2 for 35 min. After the incubation time, cells were washed with PBS twice and analyzed by flow cytometry. Diethylaminobenzaldehyde (DEAB), a specific ALDH inhibitor, was acted as negative control to establish the base line of fluorescence and to define the $ALDH^{high}$ population.

For the cell sorting, cells were resuspended at a concentration of $1*10^7$ cells/ml after staining and sorted on an Aria cell sorter. The cells were kept on ice during all the procedures. The negative

controls treated with DEAB were assessed for background fluorescence and sorting gates.

4.12 Quantitative Real-time Polymerase Chain Reaction (qRT-PCR)

Cells were collected following lysis in the trizol reagent, and total RNA was extracted with chloroform and isopropyl alcohol. Then the RNA was converted to cDNA using the RevertAid First Strand cDNA Synthesis Kit, flowing the manufacturer's guidelines. qRT-PCR was established in a total 50 μl reaction volume including 1 μl cDNA and 25 μl Power SYBR Green Master Mix running on the StepOne system in triplicate. GAPDH was employed as a reference gene and the relative expression levels were calculated using the modified delta-delta method.

The designed primer sequences of stemness-related TFs Oct3/4, Sox2, and Nanog were as follows:

Oct-3/4: Forward: GACAGGGGGAGGGGAGGAGCTAGG

Reverse: CTTCCCTCCAACCAGTTGCCCCAAAC

Sox2: Forward: GGGAAATGGGAGGGGTGCAAAAGAGG

Reverse: TTGCGTGAGTGTGGATGGGATTGGTG

Nanog: Forward: TGCGTCACACCATTGCTATTCTTC

Reverse: AATACCTCAGCCTCCAGC AGATG

4.13 Wound healing assay

In vitro wound healing assay, or so called scratch assay, is a popular, technically non-demanding and low-cost assay, which could be assessed with any readily available plates to measure the migration ability of the monolayer [55]. A confluent 24-well plate of monolayer cells was prepared, and then a "wound" was established by scraping off an area of cells using 1 ml plastic pipette tip. The non-attached cells were removed with PBS, and then covered with fresh medium containing 1% FBS and various exposures.

All the samples were incubated in a 37℃ humidified incubator with 95% air and 5% CO_2, and wound areas were captured at 0 h and 24 h after scratching with an inverted microscope at 50-fold magnification. Photographs were performed to measure the percentage of wound closure using Image J software as follows: Migrated surface area / Total surface area * 100%.

4.14 Statistical analysis

GraphPad Prism 5.0 software was used for all statistical analysis. Values were represented as mean ± standard deviation (SD). Two-group comparison was evaluated using a two-tailed t-test. Comparison among multiple groups was quantified by one-way ANOVA. Two different categorical independent variables were calculated by two-way ANOVA. A probability level of $P<0.05$ was regarded as statistically significant.

5. Results

5.1 ALDH expression is higher in spheroid-derived cells (SDCs) versus monolayer-derived cells (MDCs) in HNSCC cell lines

The Aldefluor assay has been successfully applied to detect the ALDH expression of CSCs in various cancer cells including HNSCC. Here, MDCs and SDCs from UM-SCC9, UM-SCC47, and UM-SCC11B were used to analyze ALDH enzymatic activity. As shown in Figures 1A and 1B, cells treated with the specific ALDH inhibitor DEAB were used as internal negative controls to determine the background fluorescence, and to quantify the ALDH ^{high} population. We found that SDCs established a remarkably higher percentage of ALDH ^{high} cells versus parental MDCs. The proportion of ALDH ^{high} cells in SDCs was 49.8%, 45.6%, and 33.0% in the indicated cell lines, respectively, which had an approximately 2-3 fold increased expression compared to MDCs.

5.2 Stemness-related TFs over-expressed in SDCs

Recently, one study has shown that increased expression of Sox2 and Nanog was related to radio-resistance in HNSCC, which may be associated with the CSC-specific properties [56]. To determine if SDCs derived from HNSCC cell lines also share this stemness-related feature, we measured the TFs mRNA levels in SDCs and parental MDCs. As shown in Figure 1C, the expression of Oct3/4, Sox2, and Nanog were all observed as dramatically enhanced in SDCs versus MDCs. The highest increase was found in UM-SCC47 cell line, with an average increase of 11.64, 6.97, and 11.69 fold in the indicated TFs, respectively. Taken together, these findings proved that spheroid culture could enrich the CSCs and the increased stemness-related feature, which might reasonable for maintaining cell-renewal and tumorigenesis capacity.

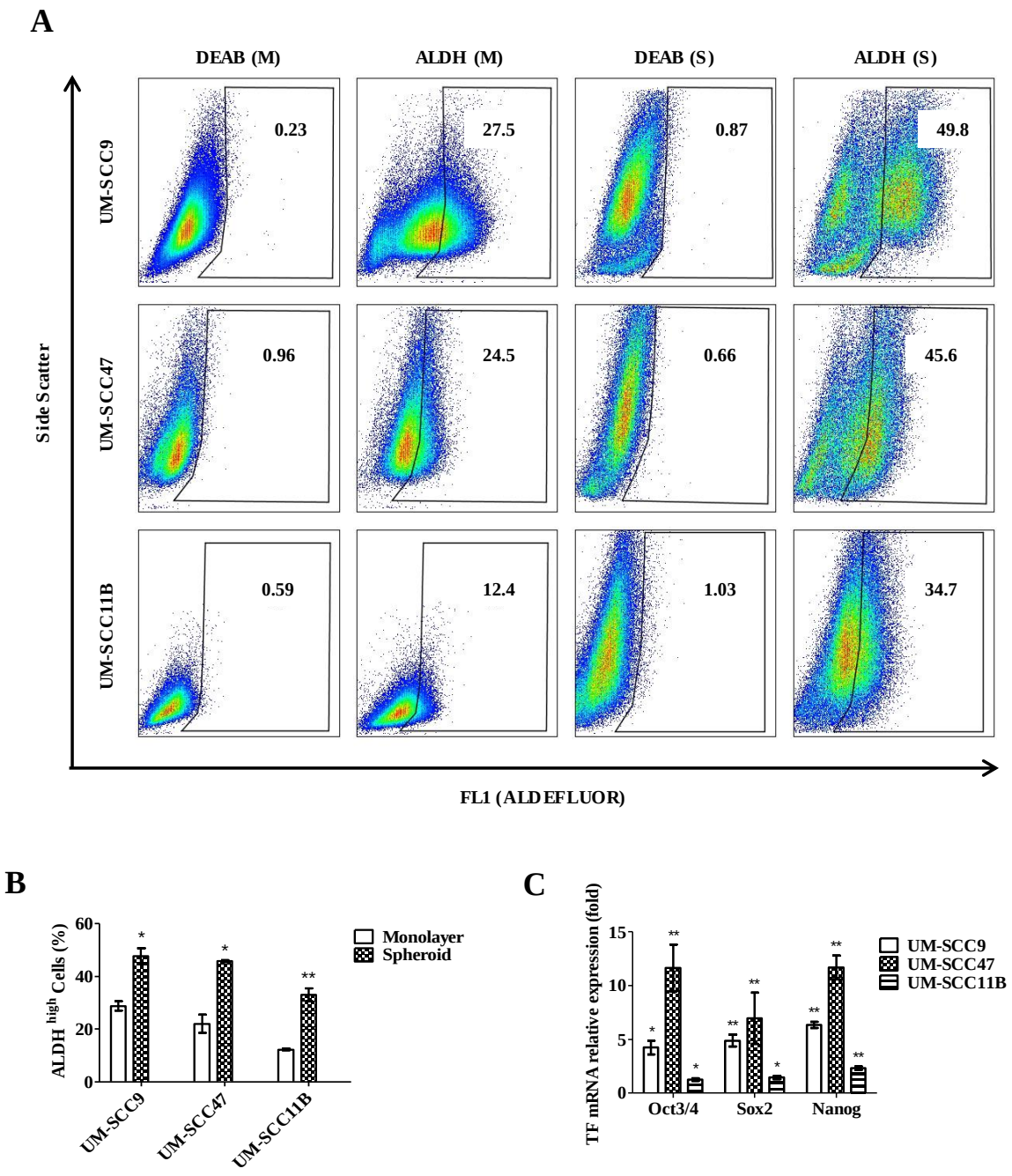

Fig. 1: Expression of ALDH and stemness-related TFs in MDCs and SDCs.

(A) Quantitation of CSCs by Aldefluor analysis. The region gate of ALDH ^{high} cells in MDCs (M) and SDCs (S) of the population is acquired by flow cytometry. DEAB, a specific ALDH inhibitor, was used as control. **(B)** Graphical representation of the statistical analysis of ALDH activity. **P*<0.05, ***P*<0.01, t-test, compared to monolayer. **(C)** Relative increase of expression of TFs by qRT-PCR of SDCs. Bars in the diagram represent the increased fold in SDCs compared to MDCs. **P*<0.05, ***P*<0.01, two-way ANOVA.

5.3 DSF exhibits dose- and time-dependent cytotoxicity in HNSCC cell lines

To explore the inhibitory effect of DSF *in vitro*, UM-SCC9, UM-SCC47, UM-SCC11B, and UT-SCC33 were used for exposure to different concentrations of DSF from 0.001 to 100 μM for 72 h. No significant cytotoxicity was observed when the concentration was lower than 1 μM (Figure 2A). Relative viability of the cells had a sharp drop at a concentration of 10 μM, and all cells were dead at 100 μM. The viability of cells was inhibited in a dose-dependent manner, and the cytotoxic effect enhanced linearly with increasing concentration of DSF in all indicated cell lines. The IC_{50} values were calculated: UM-SCC9: 13.96 μM; UM-SCC47: 13.43 μM; UM-SCC11B: 11.24 μM; and UT-SCC33: 15.06 μM.

We next measured the relationship between time and cytotoxicity by DSF in HNSCC cell lines. Cells were treated with various concentrations of DSF from 0.1 to 30 μM for 24 h, 48 h, and 72 h. We found that the average IC_{50} values in UM-SCC9 were 24.94, 18.74, and 15.32 μM; 21.91, 16.62, and 15.69 μM in UM-SCC47; 32.10, 20.05, and 14.43 μM in UM-SCC11B; and 41.95, 23.89, and 15.19 μM in UT-SCC33 in the different time courses, respectively. As shown in Figure 2B, a greatly higher value of IC_{50} than other time points was observed at 24 h in all tested cell lines. Collectively, these results indicate that DSF itself exhibits cytotoxicity in a dose- and time-dependent manner.

5.4 DSF/Cu^{2+} significantly increases cytotoxicity of HNSCC cell lines in a dose- and time-dependent manner

Although DSF alone had no obvious cytotoxicity until the concentration to 10 μM, as shown in Figure 1A, the cytotoxic effect of DSF was substantially increased with the supplement of Cu^{2+} (Figure 2C). A significant decrease was found in the relative viability of the cells at a concentration of 0.3 μM in DSF/Cu^{2+}. The DSF/Cu^{2+} complex showed remarkable increasing cytotoxicity, with the IC_{50} value of 0.24 μM in UM-SCC9, 0.193 μM in UM-SCC47, 0.267 μM in UM-SCC11B, and 0.27 μM in UT-SCC33, respectively, which is nearly 50-fold lower versus DSF alone.

We next assessed the apoptosis effect by DSF/Cu^{2+} exposure from 4 h to 72 h, with Annexin-V-FLUOS staining kit using flow cytometry. The Annexin-V^+ population (upper-right and lower-right quadrants) represent apoptotic cells. After treatment for 24 h or even longer, the dramatically enhanced cytotoxic effect was observed in all tested cell lines (Figure 2D and 2E). Taking together, these data suggested that the addition of Cu^{2+} to DSF significantly increases the

cytotoxicity compared to DSF alone in a dose- and time-dependent manner.

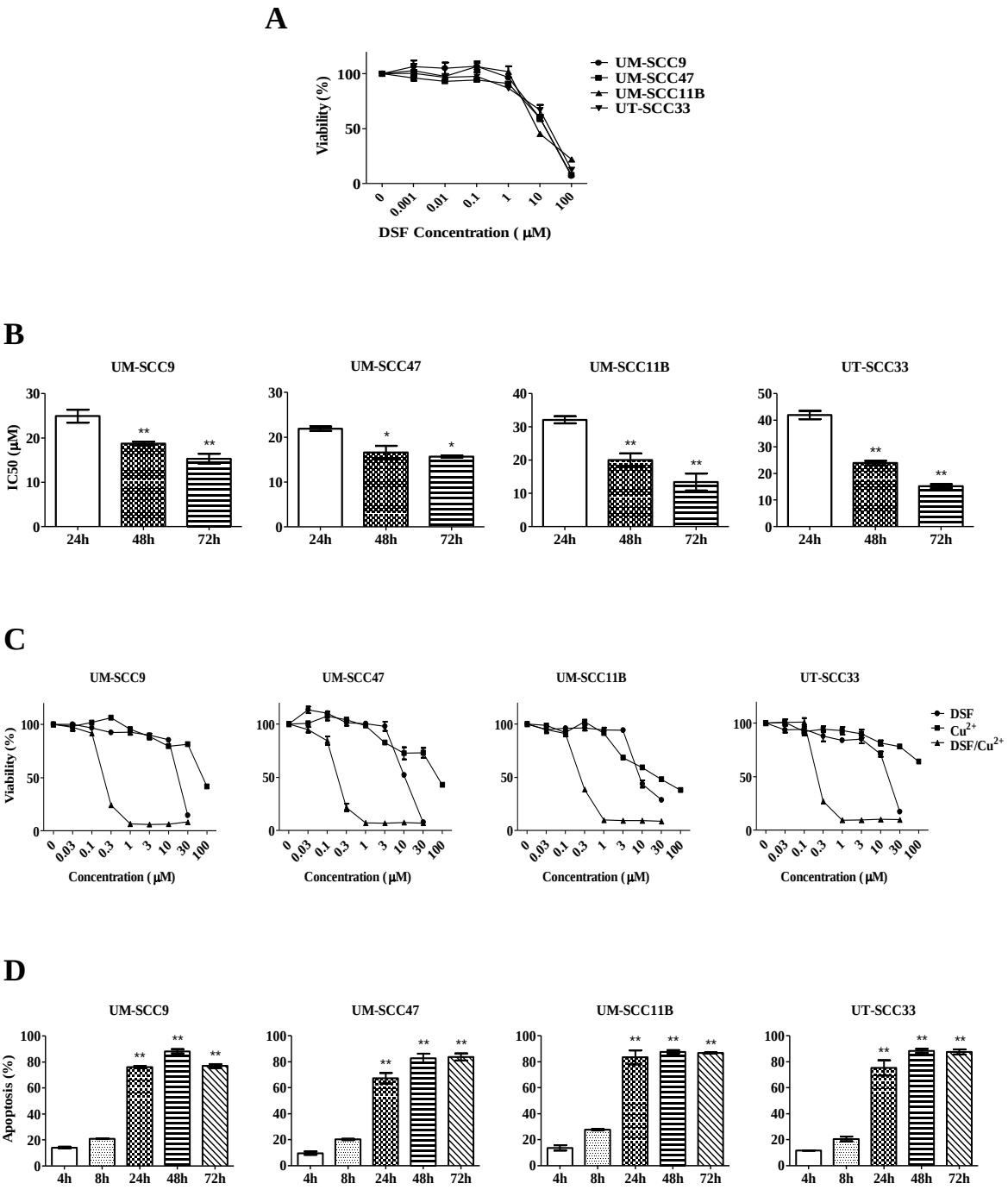

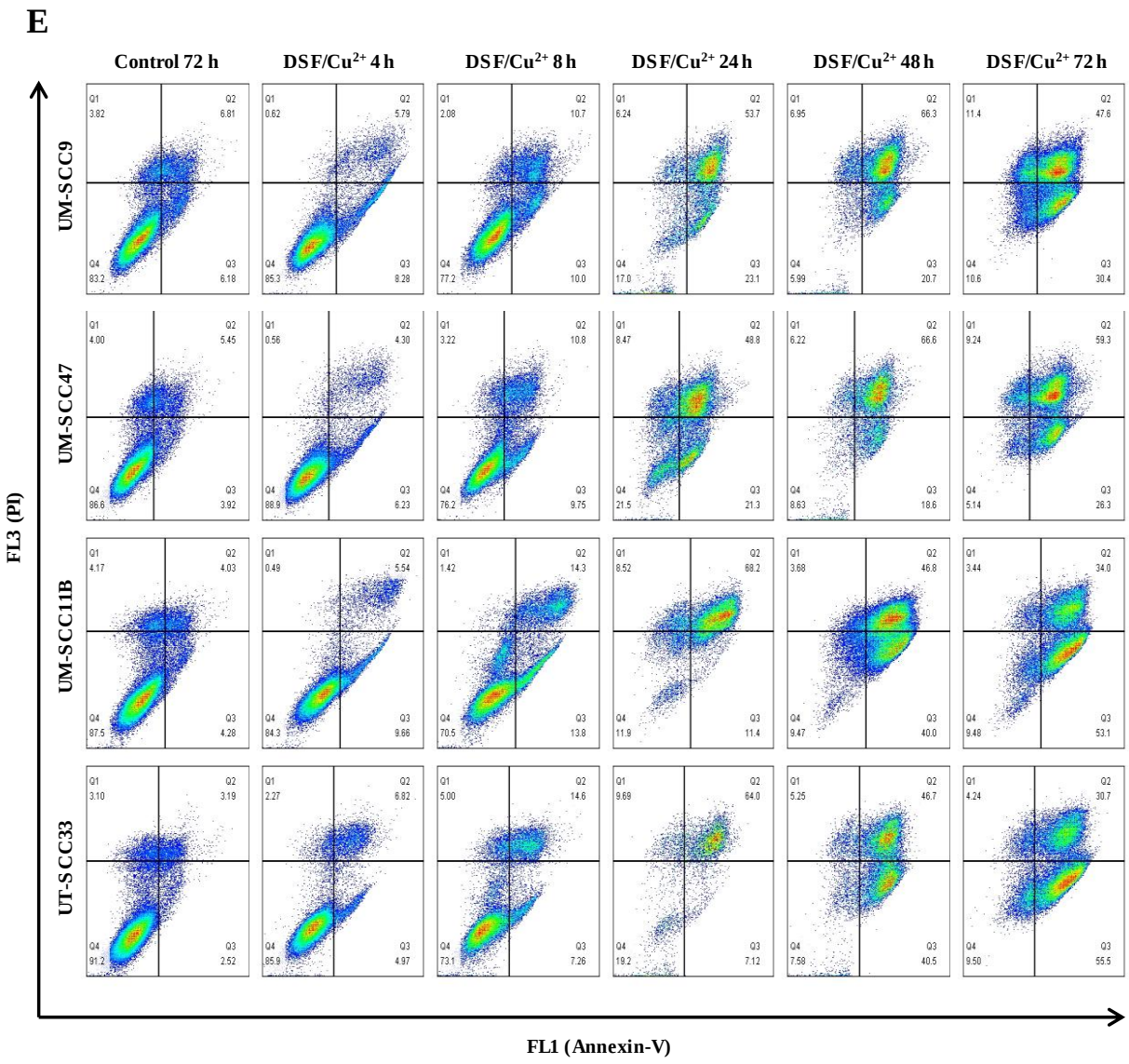

Fig. 2: Cytotoxicity of DSF or DSF/Cu^{2+} in HNSCC cell lines.

(A) Cells were treated with various concentrations of DSF for 72 h and assessed by MTT assay. **(B)** Cells were treated with various concentrations of DSF (0.1-30 µM) at the indicated time intervals. The levels of IC_{50} were detected by MTT assay. **P*<0.05, ***P*<0.01, one-way ANOVA, compared to 24 h. **(C)** Cells were treated with various combinations for 72 h and the viability was analyzed by MTT assay. **(D)** Cells were treated with DSF/Cu^{2+} (1 µM/1 µM) at the indicated time intervals. The apoptosis population was measured by Annexin-V assay. ***P*<0.01, one-way ANOVA, compared to 4 h. **(E)** The percentage of the different cell populations discriminated by Annexin-V assay is given in each quadrant (Q). The Annexin-V^{+} populations (upper-right and lower-right) represent apoptotic cells.

5.5 DSF or DSF/Cu^{2+} induces apoptosis in HNSCC cell lines

For the further measurement of cytotoxicity by DSF or DSF/Cu^{2+}, the Caspase-3 activity was analyzed using flow cytometry. Cells were treated for 48 h with various concentrations of DSF from 1 to 100 μM and DSF/Cu^{2+} complex from 0.1 to 1 μM. The no drug control treatment induced a low apoptosis percentage of 10.3%, 16.0%, 11.6%, and 10.2% in the four indicated cell lines, respectively. As is shown in Figure 3A and 3B, after exposure to 10 μM DSF, the Caspase-3 activity was induced to 24.4%, 35.3%, 32.6% and 21.6%, respectively. When the concentration of DSF was enhanced to 100 μM, a significantly high expression of Caspase-3 was detected as 82.2%, 84.0%, 88.8%, and 77.4%, respectively. Furthermore, the supplement of Cu^{2+} induced Caspase-3 activity to 61.8% in UM-SCC9, 67.7% in UM-SCC47, 74.5% in UM-SCC11B, and 53.0% in UT-SCC33, respectively. In conclusion, these findings confirm again that DSF itself enhances apoptosis in a dose-dependent manner, while the Cu^{2+} supplementation further increases this cytotoxicity.

A

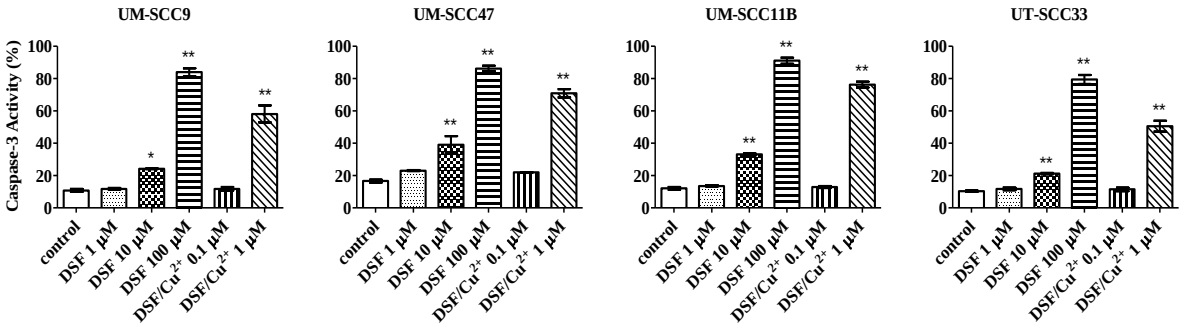

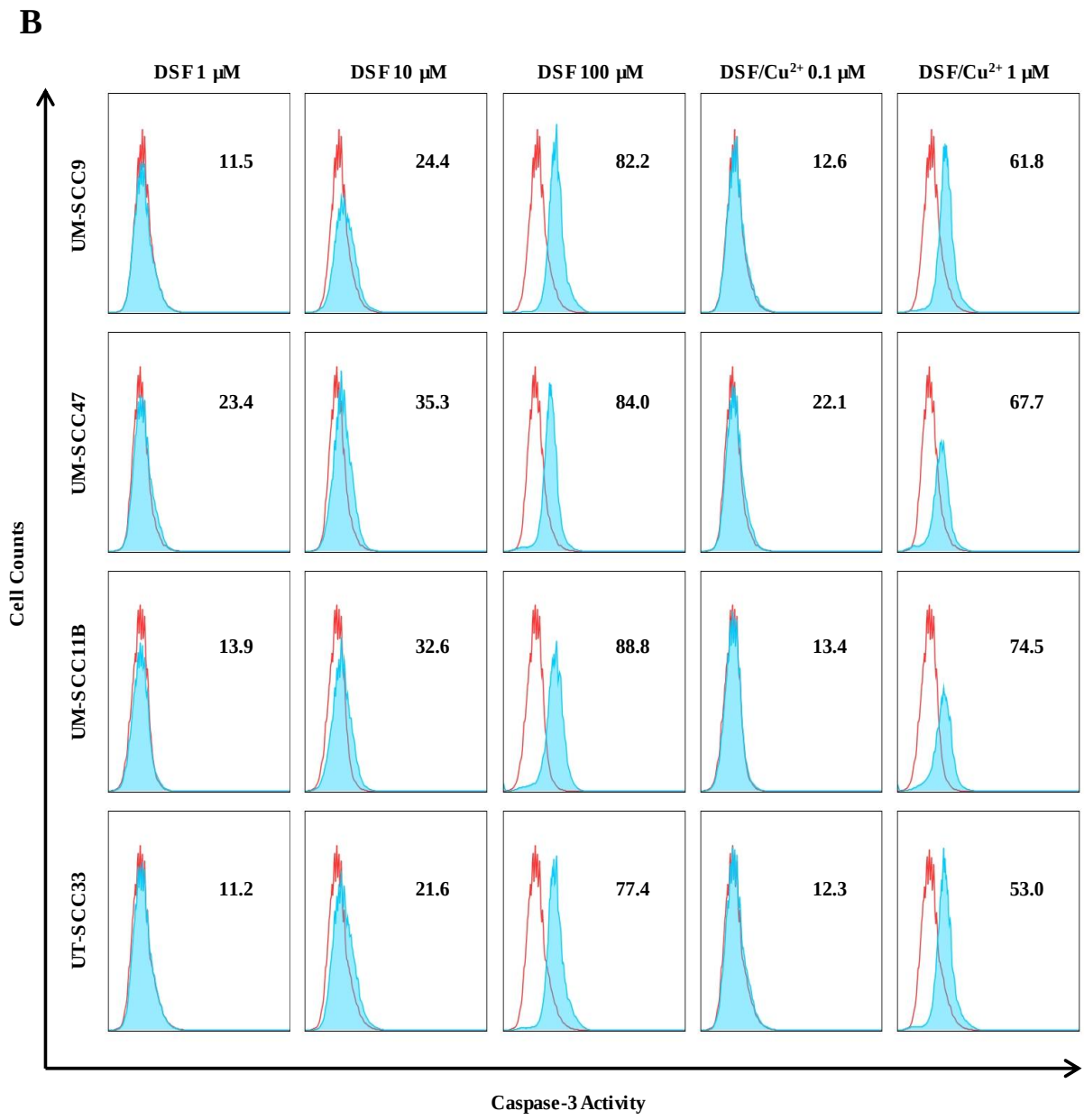

Fig. 3: DSF or DSF/Cu^{2+} induces apoptosis in HNSCC cell lines.

(A) Cells were treated with various concentrations of DSF or DSF/Cu^{2+} for 48 h, and then Caspase-3 activity was detected by flow cytometry. **P*<0.05, ***P*<0.01, one-way ANOVA, compared to control. **(B)** The Caspase-3 activity was assessed by flow cytometry. The red lines represent the controls, and the blue graphs represent the different treatments.

5.6 No significant cell cycle distribution effect by DSF or DSF/Cu^{2+} in HNSCC cell lines

The underlying mechanism of DSF or DSF/Cu^{2+} cytotoxicity is still not fully clear, therefore the cell cycle distribution was performed to measure the effect of DNA damage. Because the cell cycle phases could be compromised and disappear at high drug dosages, the concentrations used were set based on the IC_{50} values of each cell line required to avoid excessive apoptosis. Cells were exposed to various concentrations of DSF from 0.1 to 3 μM, or DSF/Cu^{2+} complex from 0.01 to 0.1 μM for 72 h, then the cell cycle was established by flow cytometry. Cells cultured without any treatment were used as controls. No significant changes were observed in the proportion of cells in the G1, S, and G2/M phases (Figure 4). Therefore, these findings demonstrate that DSF or DSF/Cu^{2+} could not act in a core role in altering the cell cycle in the chosen settings.

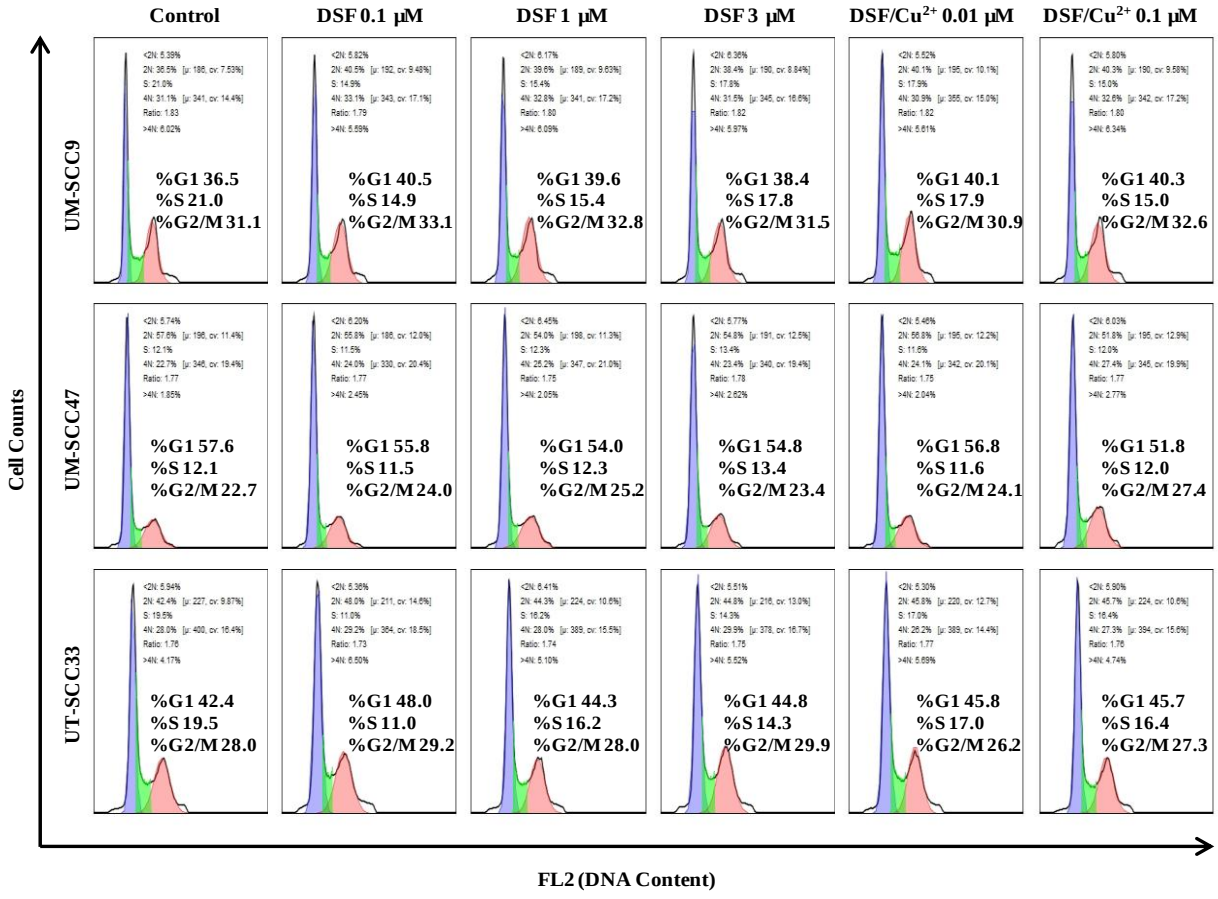

Fig. 4: No significant cell cycle distribution effect by DSF or DSF/Cu^{2+} in HNSCC cell lines.

The cell cycle distribution of cells after DSF or DSF/Cu^{2+} exposure for 72 h was detected using flow cytometry. The numbers in the graphs represent proportions as percentages of sub-G1 (<2N); G1 (2N); S-phase (S); G2/M phase (4N); and aneuploid cells (>4N).

5.7 DSF or DSF/Cu^{2+} triggers ROS generation in HNSCC cell lines

Because DSF could inhibit ALDH activity, which acts as a ROS scavenger, we hypothesize that the cytotoxic effect of DSF or DSF/Cu^{2+} might be based on the generation of ROS in HNSCC cell lines. To test this hypothesis, cells were treated with various concentrations of DSF from 1 to 100 μM, or DSF/Cu^{2+} complex from 0.1 to 1 μM. 24 h later, all cells were harvested and analyzed using flow cytometry. Similar to the induction cytotoxicity, the ROS activity was induced by increasing the concentration of DSF or DSF/Cu^{2+} (Figure 5A and 5B). After exposure to 10 μM of DSF, the ROS generation was increased to 33.1% in UM-SCC9, 35.1% in UM-SCC47, 36.9% in UM-SCC11B, and 31.2% in UT-SCC33, respectively. When the concentration was enhanced to 100 μM, a remarkably high ROS activity was detected: 98.1% in UM-SCC9, 97.6% in UM-SCC47, 97.9% in UM-SCC11B, and 98.5% in UT-SCC33, respectively. In addition, 1 μM DSF/Cu^{2+} complex could significantly increase the accumulation of ROS, which was seen to have the equivalent effect at the concentration of 100 μM DSF. Based on these observations, we conclude that the cytotoxic effect of DSF corresponds to intracellular ROS generation, while DSF/Cu^{2+} enhanced this effect nearly 100-fold compared to DSF alone.

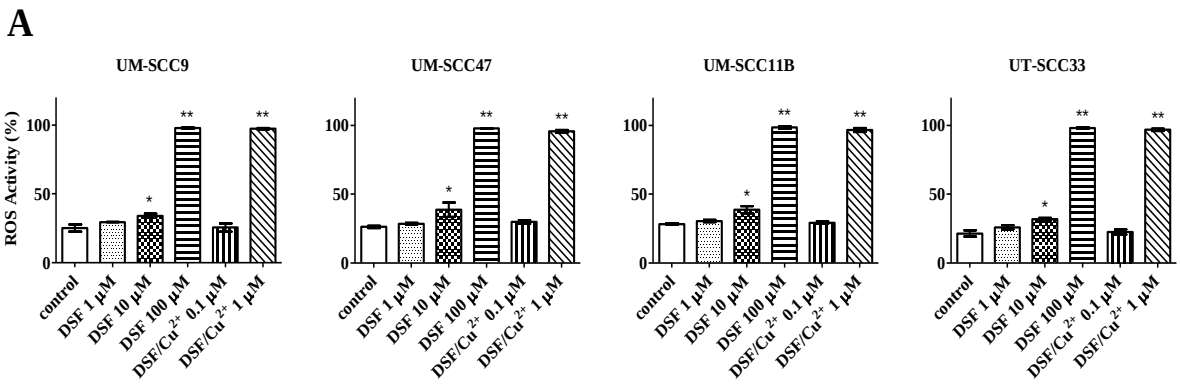

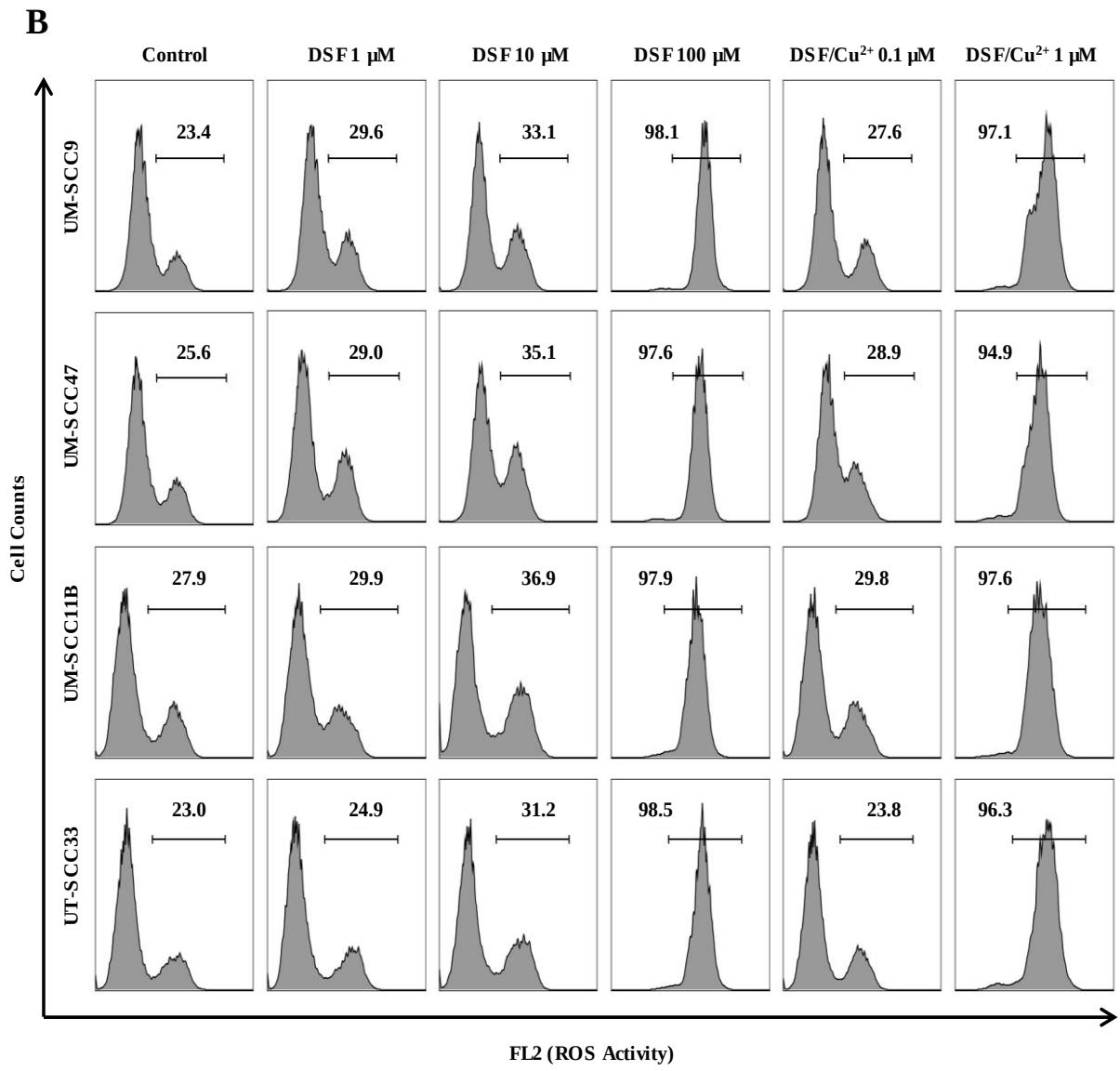

Fig. 5: DSF or DSF/Cu^{2+} triggers ROS generation in HNSCC cell lines.

(A) Cells were treated with various concentrations of DSF or DSF/Cu^{2+} for 24 h, and then ROS activity was detected using flow cytometry. **P*<0.05, ***P*<0.01, one-way ANOVA, compared to control. **(B)** The numbers in the graphs represent the ROS activity.

5.8 DSF or DSF/Cu^{2+} inhibits ALDH enzyme activity in SDCs

To evaluate the effective targeting of CSCs by DSF or DSF/Cu^{2+}, the ALDH activity was determined in SDCs derived from tested HNSCC cell lines. As shown in Figure 6A and 6B, cells were treated with 10 μM DSF or 0.15 μM DSF/Cu^{2+} for 72 h, and then the percentage of ALDH ^{high} cells was significantly decreased from 59.8% to 33% and 30.0% in UM-SCC9, 41.8% to 21.2% and 20.0% in UM-SCC47, and 44.5% to 30.8% and 29.4% in UM-SCC11B, respectively. DEAB, a specific ALDH inhibitor, acted as a negative control to establish the ALDH ^{high} population and the background of fluorescence intensity.

5.9 DSF or DSF/Cu^{2+} inhibits the expression of stemness-related TFs in SDCs

As we had demonstrated that the SDCs expressed significantly higher levels of stemness-related TFs in HNSCC cell lines, we further investigated the inhibition effect of DSF or DSF/Cu^{2+} on SDCs by analyzing the CSC markers of Oct3/4, Sox2 and Nanog. From the analysis described in Figure 6C, it is clear that the TFs expression is remarkably decreased compared to untreated samples after treatment with 10 μM DSF or 0.15 μM DSF/Cu^{2+} for 72 h. The highest drop was detected in UM-SCC9, with an average of 0.33 or 0.39 fold in Oct3/4; 0.20 or 0.63 fold in Sox2; and 0.39 or 0.25 fold in Nanog, in DSF or DSF/Cu^{2+}, respectively. Collectively, these results provide strong evidence that DSF reduce CSC-associated features, and the addition of Cu^{2+} could increase this inhibition, leading to therapy sensitizing effects.

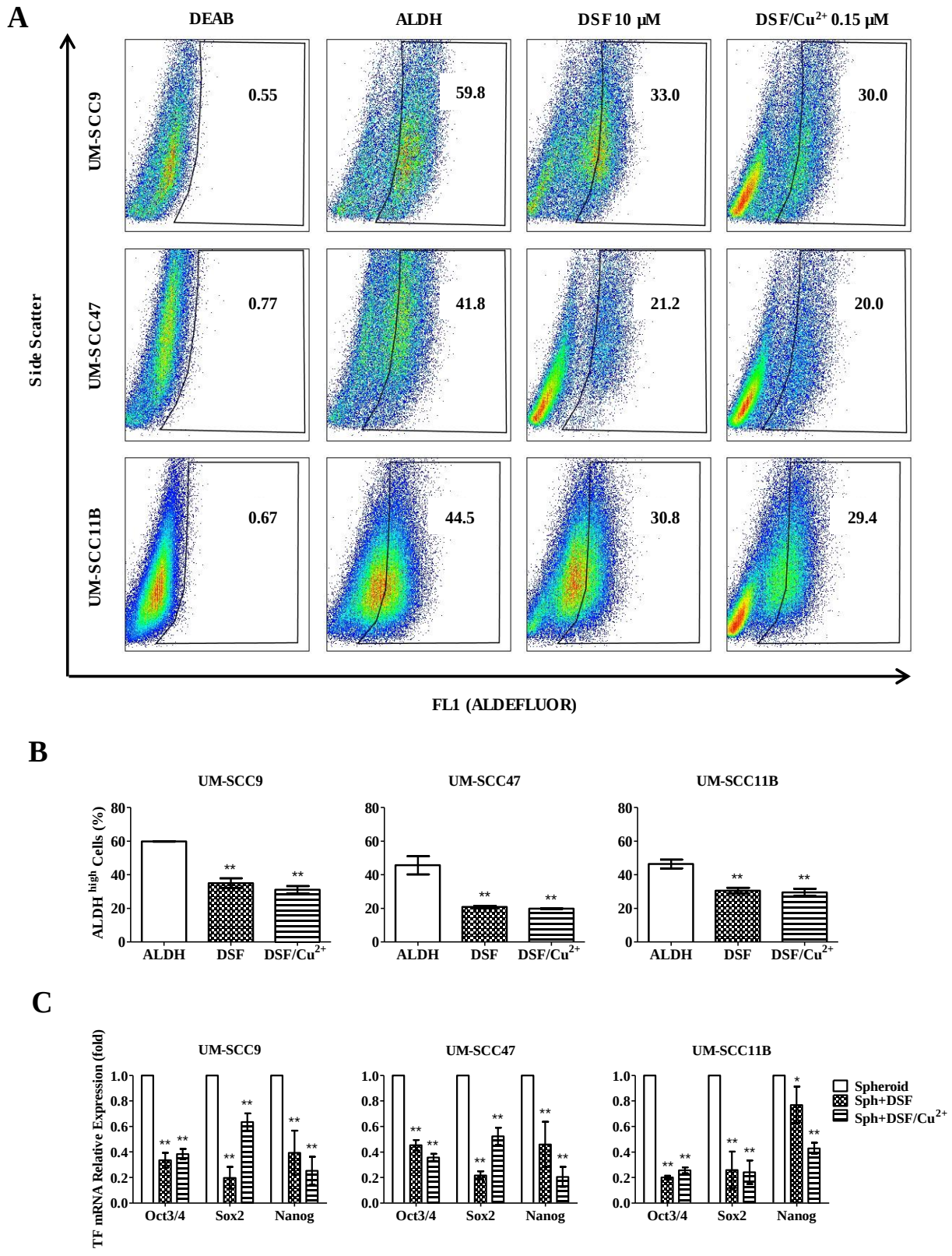

Fig. 6: DSF or DSF/Cu^{2+} inhibits ALDH expression and stemness-related TFs expression of SDCs in HNSCC cell lines.

(A) The ALDH expression of SDCs was measured by Aldefluor analysis after DSF or DSF/Cu^{2+}

exposure for 72 h. DEAB, a specific ALDH inhibitor, was used as control. The numbers in the graph represent percent of ALDH ^{high} cells in the population acquired by flow cytometry. **(B)** Graphical representation of the statistical analysis of ALDH activity. $^{**}P<0.01$, one-way ANOVA, compared to untreated control. **(C)** SDCs were exposed to DSF 10 μM or DSF/Cu^{2+} 0.15 μM for 72 h, mRNA was quantified for expression of the indicated panel of TFs. $^{*}P<0.05$, $^{**}P<0.01$, two-way ANOVA, compared to untreated control.

5.10 Inhibition of colony formation by DSF or DSF/Cu^{2+} in HNSCC cell lines

The clonogenicity assay was established to explore the cellular reproductive stemness capacity of cancer cells after various exposures. In this study, we investigated whether DSF or DSF/Cu^{2+} could inhibit this clonogenic capacity. Compared to no-drug treatment controls, the numbers of colony-formation units were decreased from an average of 145 to 72 and 70 in UM-SCC9, 140 to 80 and 68 in UM-SCC47, and 138 to 75 and 67 in UM-SCC11B, respectively, after exposure to 3 μM DSF or 0.1 μM DSF/Cu^{2+} complex in all tested cell lines (Figure 7A). This result may be due to a slower growth of the surviving cells, leading to lower cell amounts, which do not reach the minimum standard that defines a colony. Taken together, these findings demonstrate that DSF could able to suppress clonogenicity in HNSCC cell lines and the Cu^{2+} supplement could reduce the concentration of DSF to increase this effect.

5.11 Inhibition of spheroid formation by DSF or DSF/Cu^{2+} in HNSCC cell lines

Spheroid-derived cells (SDCs) are considered to enrich CSCs or cells with stemness-related characteristics. To investigate the proliferative potential of CSCs and the ability of epithelial cells to grow anchorage independently, spheroid formation assay was performed. As shown in Figure 7B, a large amount of spheroids were grown in untreated control cells in all tested cell lines. To gain a better understanding of the inhibition ability of DSF or DSF/Cu^{2+}, cells were treated with 10 μM DSF or 0.15 μM DSF/Cu^{2+} complex for 3-5 days and photographs were taken at 50-fold magnification. After the incubation time, small and inattentive spheroids and loose cellular aggregates were captured, this indicated that the ability of spheroid formation was significantly reduced. The average spheroid number was remarkably decreased from 39 to 18 and 20 in UM-SCC9; from 42 to 21 and 24 in UM-SCC47; and from 36 to 19 and 17 in UM-SCC11B, compared to untreated controls, respectively. These results suggest that stemness inhibition could be achieved by DSF or DSF/Cu^{2+} exposure to reduce the self-renewal capacity in HNSCC cell lines.

5.12 Inhibition of migratory ability by DSF or DSF/Cu^{2+} in HNSCC cell lines

Cell migration plays a core role in various pathologic and physiologic processes across varieties of disciplines of biology including wound healing, inflammation, tumor growth and differentiation [57]. Consequently, we further evaluated whether DSF or DSF/Cu^{2+} exposure could inhibit cell migration ability in HNSCC cell lines using the wound healing assay. After exposure to 10 μM DSF or 0.15 μM DSF/Cu^{2+} complex, the percentage of wound area closure was analyzed at an interval 20 h in UM-SCC9 and UM-SCC47, and at 24 h in UM-SCC11B. Figure 7C summaries the noteworthy inhibitions of migration ability in all tested cell lines. The no-drug treated cells had closed the scratch by 71.85% in UM-SCC9, 73.78% in UM-SCC47, and 73.51% in UM-SCC11B. However, after treatment with DSF or DSF/Cu^{2+}, the cells reduced the percentage of wound closure by only 42.1% and 43.49% in UM-SCC9; by 45.86% and 43.00% in UM-SCC47; and by 43.97% and 41.2% in UM-SCC11B, respectively, which demonstrated that DSF or DSF/Cu^{2+} could inhibit the migration ability of cells *in vitro*.

A

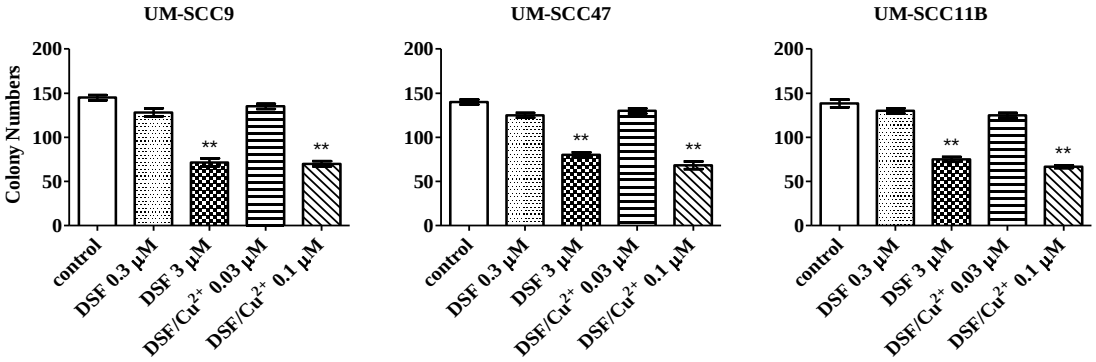
UM-SCC9
UM-SCC47
UM-SCC11B
Colony Numbers
200
150
100
50
0
**
control
DSF 0.3 μM
DSF 3 μM
DSF/Cu2+ 0.03 μM
DSF/Cu2+ 0.1 μM

B

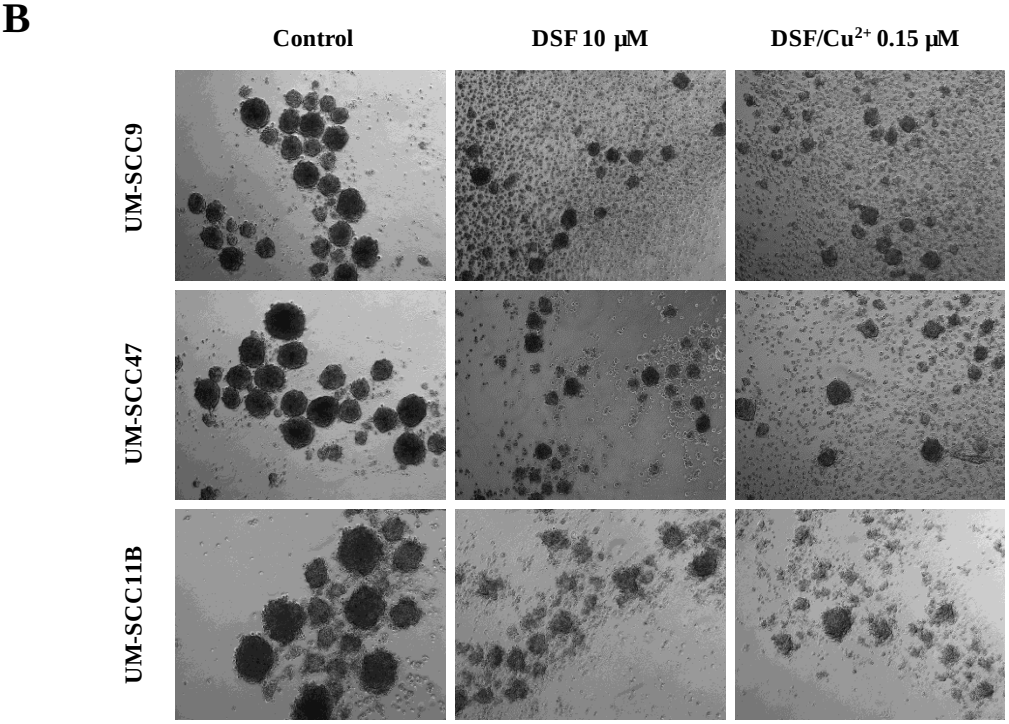
Control
DSF 10 μM
DSF/Cu2+ 0.15 μM
UM-SCC9
UM-SCC47
UM-SCC11B

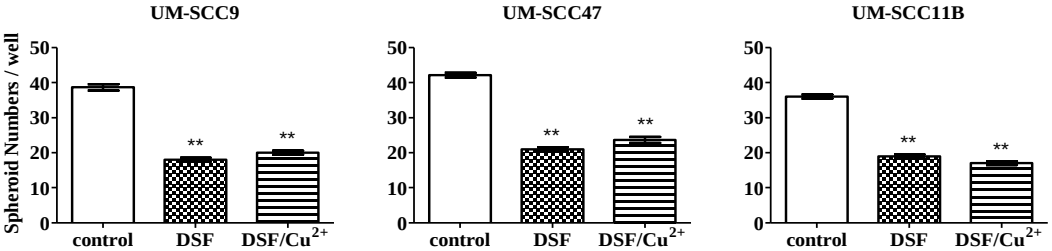
UM-SCC9
UM-SCC47
UM-SCC11B
Spheroid Numbers / well
50
40
30
20
10
0
**
control
DSF
DSF/Cu2+

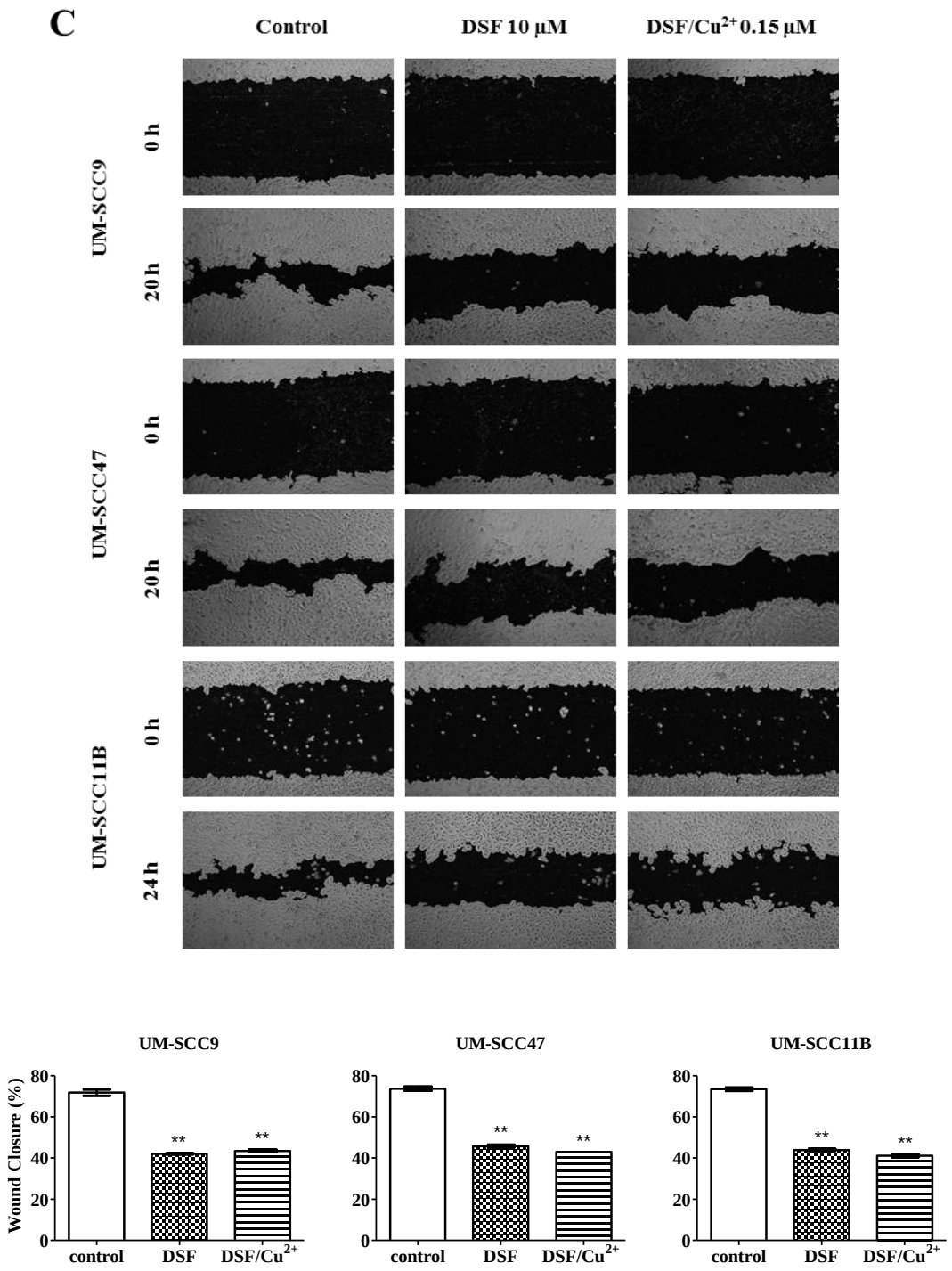

Fig. 7: DSF or DSF/Cu^{2+} inhibits colony formation, spheroid formation and migratory ability in HNSCC cell lines.

(A) Cells were treated with various concentrations of DSF or DSF/Cu^{2+} for 24 h and then reseeded in drug-free medium for 9-12 days. Colonies with minimum of 50 cells or more were counted. Graphical representation of the statistical analysis. $^{**}P<0.01$, one-way ANOVA,

compared to control. **(B)** Cells were exposed to DSF or DSF/Cu^{2+} for 72 h and representative images are shown (x50 magnification). The histogram shows the statistical analysis of spheroid numbers. ***P*<0.01, one-way ANOVA, compared to control. **(C)** Representative pictures indicate the migratory cells under different treatment conditions and time points (x 50 magnification). The graphical representation shows the statistical analysis of migratory ability. ***P*<0.01, one-way ANOVA, compared to control.

5.13 Increase of colony formation, spheroid formation, and decrease of ROS activity in ALDH ^{high} cells versus ALDH ^{low} cells

Since ALDH has been reported previously as an important stem cell marker in HNSCC, the FACS-sorted ALDH ^{high} and ALDH ^{low} population were treated and analyzed for further investigation of CSC-features. The colony formation and the spheroid formation were established to measure the cell-renewal capacity of ALDH ^{high} and ALDH ^{low} cells. As shown in Figure 8A and 8B, the ALDH ^{high} population could form significantly greater numbers of colonies and spheroids compared to the ALDH ^{low} population in standard culture conditions, which indicates a property relating to tumor initiating ability.

Furthermore, we evaluated the ROS activity in both ALDH ^{high} and ALDH ^{low} sorted cells. As shown in Figure 8C, ALDH ^{high} cells indicated a lower basal level of ROS accumulation because of higher expression of ALDH, which is a ROS scavenger to protect cells against oxidative stress. Additional, this difference between two population cells also suggested that ALDH ^{low} cell with rapid metabolism while ALDH ^{high} cells were more quiescent. In conclusion, these findings indicate that ALDH activity plays an essential role in HNSCC CSCs.

5.14 DSF overcomes the resistance of cisplatin in ALDH ^{high} cells

To investigate the significance role of ALDH in chemo-resistance, the relative viability of FACS-sorted ALDH ^{high} and ALDH ^{low} cells were measured after treated with different concentrations of cisplatin. A significant difference of growth capacity between two populations was detected in Figure 8D. The ALDH ^{high} cell fractions showed more resistant to cisplatin treatment, particularly starting from lower concentration (1.25 μM), compared to the ALDH ^{low} cells. Nevertheless, when combined with 5 μM DSF, the cytotoxic effect of cisplatin in ALDH ^{high} cells was greatly enhanced. In conclusion, these findings prove that DSF could target HNSCC CSCs in the specifically highly enriched ALDH ^{high} population and increase the effectiveness treatment of cisplatin leading to chemo-sensitizing.

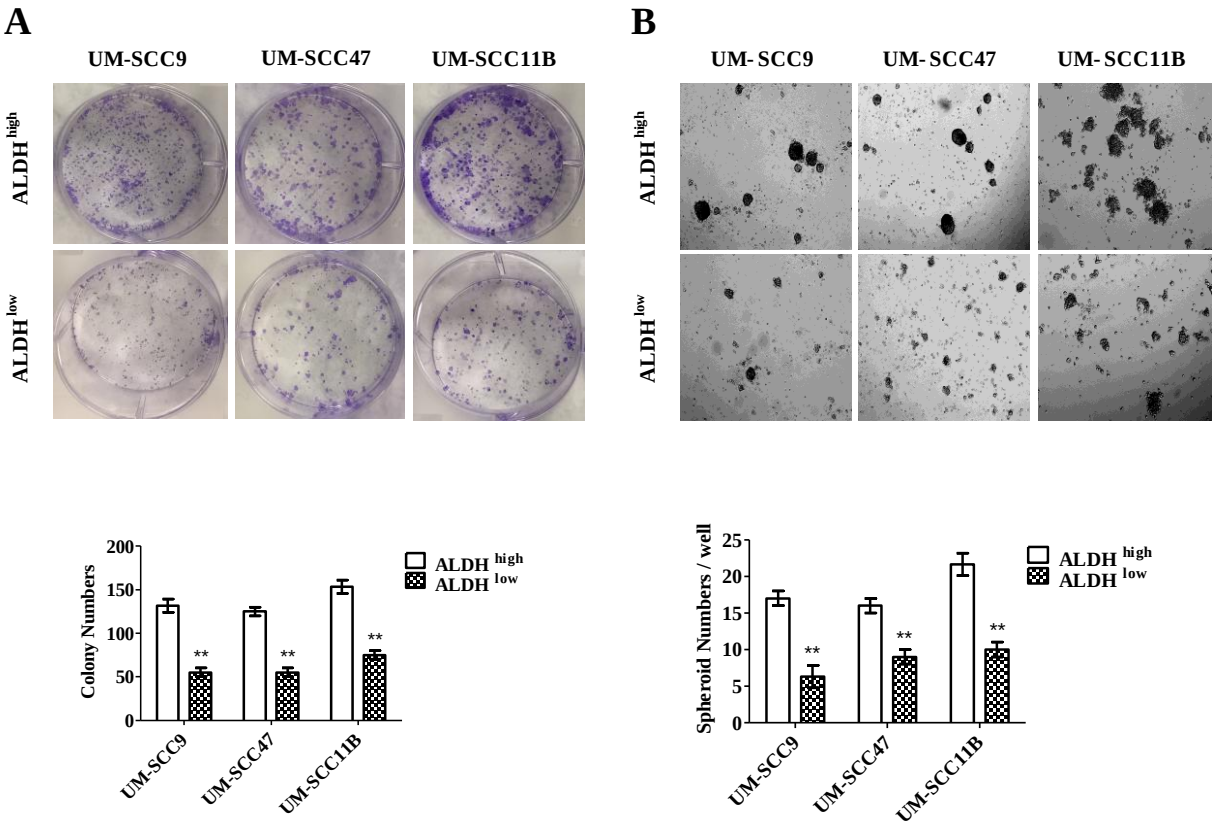
A
UM-SCC9
UM-SCC47
UM-SCC11B
ALDH high
ALDH low
B
UM- SCC9
UM- SCC47
UM- SCC11B
ALDH high
ALDH low
Colony Numbers
ALDH high
ALDH low
Spheroid Numbers / well
ALDH high
ALDH low
C
UM-SCC9
UM-SCC47
UM-SCC11B
29.0
15.7
27.0
53.3
34.9
52.8
Cell Counts
FL2 (ROS Activity)
ROS Activity (%)
ALDH high
ALDH low
D
UM-SCC9 Cisplatin
UM-SCC9 ALDH high
UM-SCC47 ALDH high
Viability (%)
Concentration (μM)
ALDH high
ALDH low
Cisplatin
Cisplatin+DSF

Fig. 8: Analysis of stemness, ROS activity, and cisplatin sensitivity in ALDH-sorted cells.

(A) ALDH ^{high} and ALDH ^{low} cells were cultured for 9-12 days. Colonies with minimum of 50 cells or more were calculated. Histogram shows the statistical analysis of colony numbers. $^{**}P<0.01$, t-test, compared to ALDH ^{high} cells. **(B)** ALDH ^{high} and ALDH ^{low} cells were cultured for 3-5 days. The graphical representation of the statistical analysis shows the spheroid numbers. $^{**}P<0.01$, t-test, compared to ALDH ^{high} cells. **(C)** ROS activity of ALDH ^{high} and ALDH ^{low} cells was detected by flow cytometry. $^{**}P<0.01$, t-test, compared to ALDH ^{high} cells. **(D)** ALDH ^{high} and ALDH ^{low} cells were exposed to various concentrations of cisplatin, or in a combination of 5 μM DSF for 72 h and the viability was assessed by MTT assay.

5.15 DSF and cisplatin combination induce synergistically cytotoxicity

The combination of drugs could abolish treatment resistance compared to a single compound, thus it is meaningful to define the drugs that act synergistically. Next, we attempted to assess whether DSF could improve the sensitivity of HNSCC cell lines to cisplatin treatment. As shown in Figure 9A, when 5 μM DSF was added to different concentrations of cisplatin, the cytotoxic effect was increased substantially.

To gain a better understating of the essence of these results, the combination index (CI) according to Chou-Talalay method was performed. As shown in Table 1, the combination of DSF and cisplatin established a synergistic effect in all tested HNCC cell lines at a broad level of ED_{50} and ED_{75} with CI<1. Taken together, these findings demonstrate that DSF decreases cellular viability synergistically and improves the cytotoxic effect of cisplatin treatment.

5.16 DSF or DSF/Cu^{2+} abolishes cisplatin-induced G2/M phase arrest

Based on the combination cytotoxicity affection in the previous experiments, we hypothesized that the mechanism might be related to the abolishment of the G2/M phase following the drug treatment. Therefore, the cell cycle distribution was performed after 48 h of exposure to cisplatin in the presence of DSF or DSF/Cu^{2+}. As shown in Figure 9B and 9C, cisplatin (0.3 μM for UM-SCC9 and UM-SCC47, 0.6 μM for UT-SCC33) increased G2/M activation, which was due to more cell blocking in the G2/M phase, and less in G1/G0. We observed a prominent G2/M phase increase from 30.0% to 52.9% in UM-SCC9, 31.3% to 56.4% in UM-SCC47, and 23.6% to 54.7% in UT-SCC33, respectively. Nevertheless, when cells combined with 5 μM DSF or 0.1 μM DSF/Cu^{2+}, a significant reduction of the G2/M phase was recognized, with a parallel induction of

cells in the G1 phase. A dramatic attenuation was detected from 52.9% to 41.2% and 42.2% in UM-SCC9, 56.4% to 43.1% and 44.9% in UM-SCC47, and 54.7% to 42.3% and 45.6% in UT-SCC33, respectively. Therefore, these results suggest that DSF or DSF/Cu^{2+} could abolish cisplatin-induced arrest, which is responsible for lower cell blocking in the G2/M phase resulting in apoptosis induction.

Table 1: Combination treatment with DSF and cisplatin results in synergistic cytotoxic effect in HNSCC cell lines.

Cisplatin + DSF	**Combination Index [a] at**	
	ED50	ED75
UM-SCC 9	0.560	0.447
UM-SCC47	0.676	0.624
UM-SCC11B	0.543	0.551
UT-SCC33	0.645	0.507

a) Combination Index (CI) for the combination of DSF and cisplatin. CI=1 indicates an additive effect; CI<1 indicates a synergistic effect; CI>1 indicates an antagonistic effect.

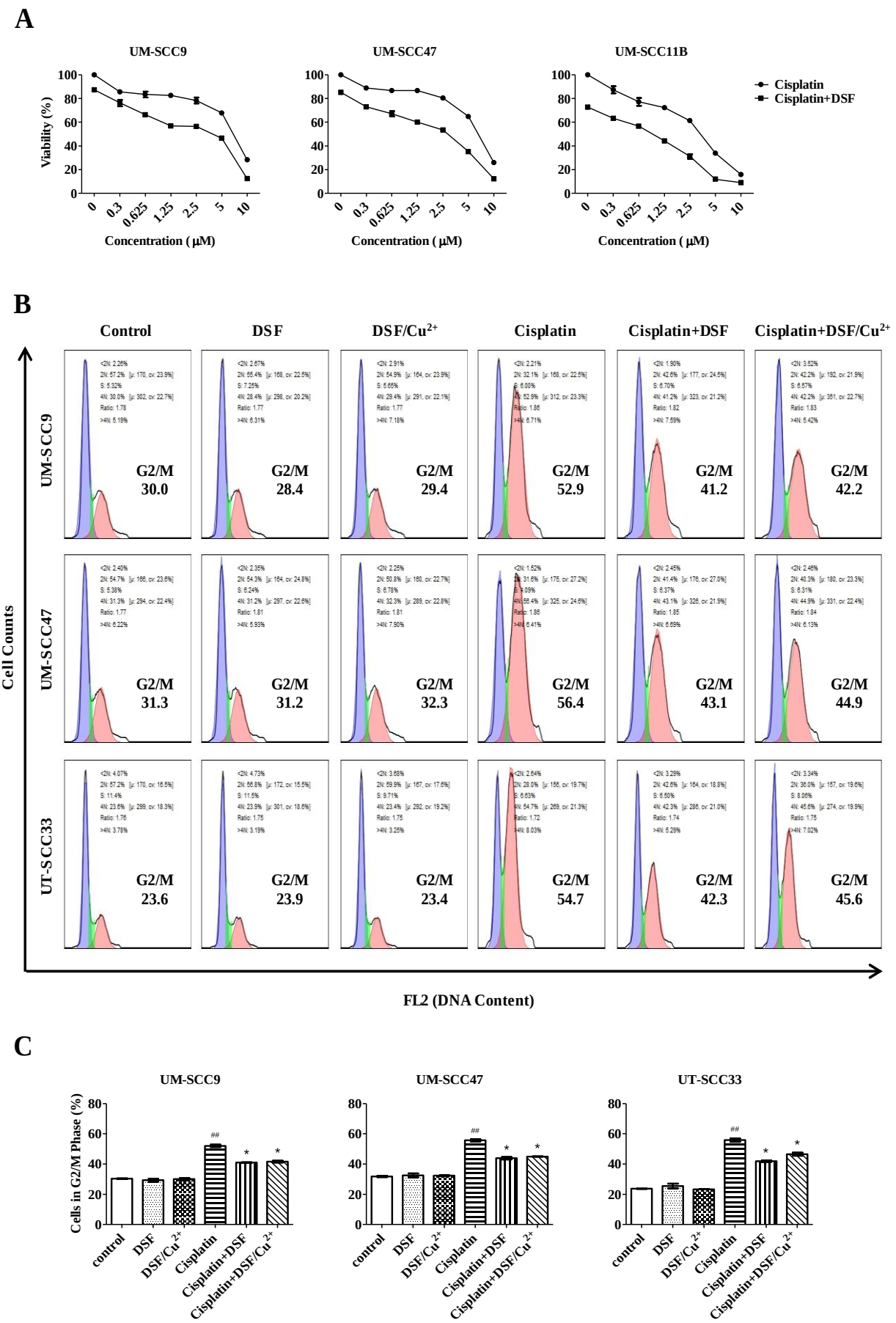
A
UM-SCC9
UM-SCC47
UM-SCC11B
Viability (%)
Concentration (μM)
Cisplatin
Cisplatin+DSF
B
Control
DSF
DSF/Cu2+
Cisplatin
Cisplatin+DSF
Cisplatin+DSF/Cu2+
UM-SCC9
UM-SCC47
UT-SCC33
G2/M 30.0
G2/M 28.4
G2/M 29.4
G2/M 52.9
G2/M 41.2
G2/M 42.2
G2/M 31.3
G2/M 31.2
G2/M 32.3
G2/M 56.4
G2/M 43.1
G2/M 44.9
G2/M 23.6
G2/M 23.9
G2/M 23.4
G2/M 54.7
G2/M 42.3
G2/M 45.6
Cell Counts
FL2 (DNA Content)
C
UM-SCC9
UM-SCC47
UT-SCC33
Cells in G2/M Phase (%)
control
DSF
DSF/Cu2+
Cisplatin
Cisplatin+DSF
Cisplatin+DSF/Cu2+

Fig. 9: Combination with DSF or DSF/Cu^{2+} and cisplatin in HNSCC cell lines.

(A) Cells were treated with various concentrations of cisplatin and 5 μM DSF for 72 h and the cytotoxic effect was determined by MTT assay. **(B)** Cells were treated with DSF (5 μM), DSF/Cu^{2+} (0.1 μM), cisplatin (UM-SCC9 and UM-SCC47: 0.3 μM; UT-SCC33: 0.6 μM) or a combination of both for 48 h. The cell cycle distribution was detected by flow cytometry. The numbers in the graph represent proportions as a percentage of sub-G1 (<2N); G1 (2N); S-phase (S); G2/M phase (4N); and aneuploid cells (>4N). **(C)** The percentage of cells in the G2/M phase is compared. $^{\#\#}P<0.01$: cisplatin vs. control; $^{*}P<0.05$: cisplatin vs. cisplatin+DSF or cisplatin+DSF/Cu^{2+}; one-way ANOVA.

5.17 Radio-sensitizing effect of DSF or DSF/Cu^{2+}

The cellular viability was evaluated to investigate the combination cytotoxicity of IR and DSF or DSF/Cu^{2+}. Cells were pre-treated with various concentrations of DSF or DSF/Cu^{2+}, then exposed to IR (10 Gy) and subsequently cultured for 72 h. The combined treatment was compared, and the results are shown in Figure 10A. When a combination of DSF or DSF/Cu^{2+} with IR was applied, the dose response curves showed a significantly enhanced cytotoxic effect.

Furthermore, to determine whether DSF or DSF/Cu^{2+} could potentiate a radio-sensitizing effect in HNSCC cell lines, the cells pre-treated with 1 μM DSF or 0.1 μM DSF/Cu^{2+} were exposed to a graded dosage of IR. Cell survival fraction was performed using colony formation, which is a primary assay to define cellular “reproductive death” after drug exposure. As shown in Figure 10B, combination with DSF or DSF/Cu^{2+} and IR inhibits cell survival at the indicated dosage. In conclusion, these findings indicate that DSF or DSF/Cu^{2+} could increase the cytotoxicity of IR leading to radio-sensitizing effects.

5.18 Combination of DSF or DSF/Cu^{2+} attenuate IR-induced G2/M phase arrest

One of the hallmarks of cellular responses to IR is the activation of the G2/M checkpoint to prevent cells with DNA damage from entering mitosis. Firstly, we investigated the cell cycle distribution with the increasing dosage of IR. As is shown in Figure 10C, after a relatively high dosage exposure, starting from 10 Gy, large amounts of cells were blocked in the G2/M phase (41.9% in UM-SCC9, 40.8% in UM-SCC47, and 45.4% in UM-SCC11B, respectively) compared to 0 Gy controls (28.2% in UM-SCC9, 27.7% in UM-SCC47, and 30.6% in UM-SCC11B, respectively).

To explore the potential nature of DSF or DSF/Cu^{2+} sensitized cells to IR, cell cycle distribution analysis was performed after combination exposure. Cells were pre-treated with 5 μM DSF or 0.1 μM DSF/Cu^{2+} following exposure at 10 Gy IR. As shown in Figure 10D and 10E, a dramatic G2/M phase activation was detected after 48 h of IR with an increase from 27.7% to 53.6% in UM-SCC9 and from 28.2% to 50.0% in UM-SCC47, respectively, with a concomitant decrease in the G1 phase as well. However, when combined with DSF or DSF/Cu^{2+}, it resulted in reducing the G2/M phase from 53.6% to 40.2% and 41.9% in UM-SCC9, and from 50.0% to 39.5% and 39.7% in UM-SCC47, respectively. Taken together, these results provide strong evidence that DSF or DSF/Cu^{2+} could attenuate IR-induced G2/M phase arrest where checkpoints in the cell cycle or DNA repair signaling pathways might be involved.

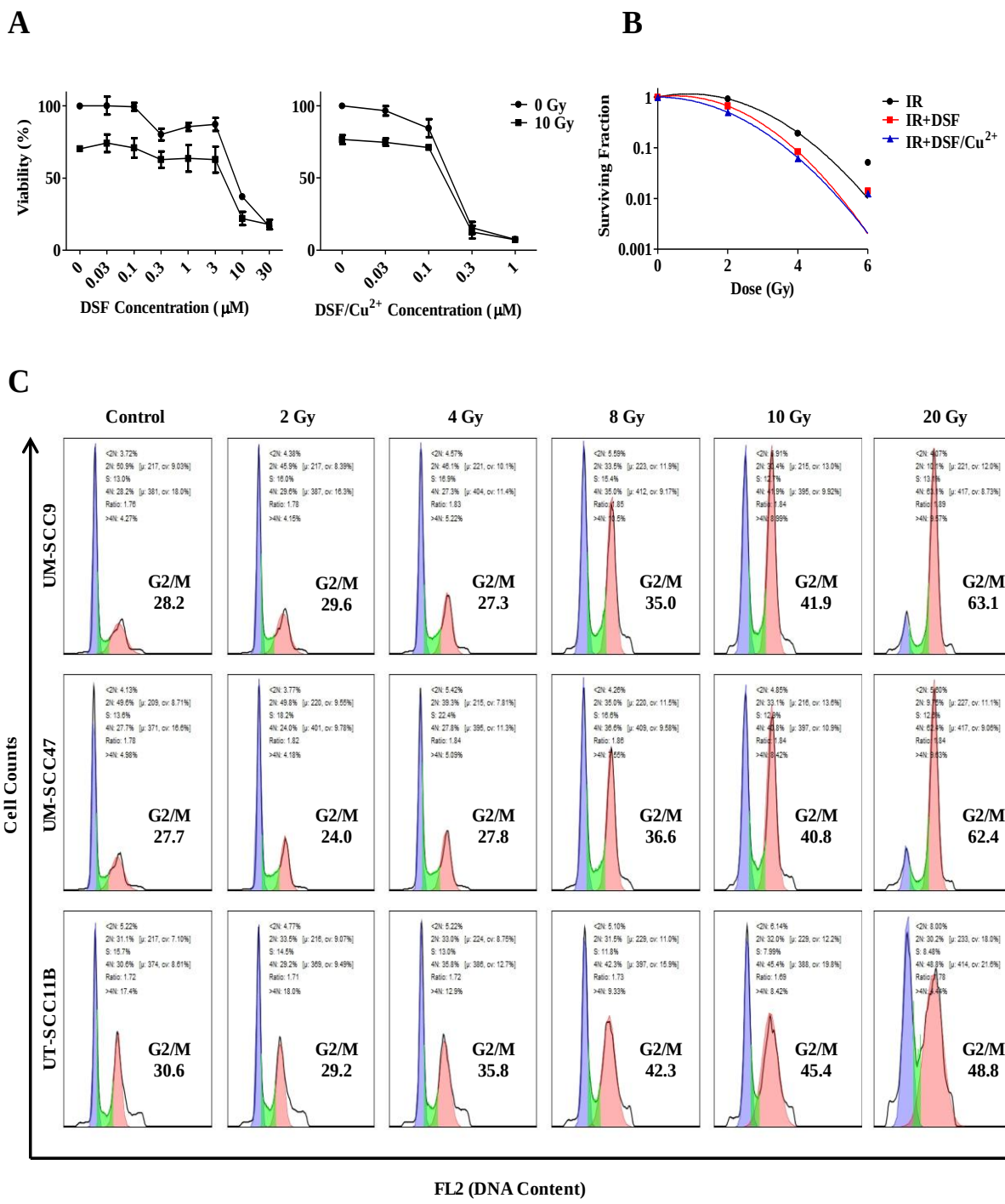
A
B
C
Viability (%)
DSF Concentration (μM)
DSF/Cu2+ Concentration (μM)
0 Gy
10 Gy
Surviving Fraction
Dose (Gy)
IR
IR+DSF
IR+DSF/Cu2+
Control
2 Gy
4 Gy
8 Gy
10 Gy
20 Gy
UM-SCC9
UM-SCC47
UT-SCC11B
Cell Counts
FL2 (DNA Content)
G2/M 28.2
G2/M 29.6
G2/M 27.3
G2/M 35.0
G2/M 41.9
G2/M 63.1
G2/M 27.7
G2/M 24.0
G2/M 27.8
G2/M 36.6
G2/M 40.8
G2/M 62.4
G2/M 30.6
G2/M 29.2
G2/M 35.8
G2/M 42.3
G2/M 45.4
G2/M 48.8

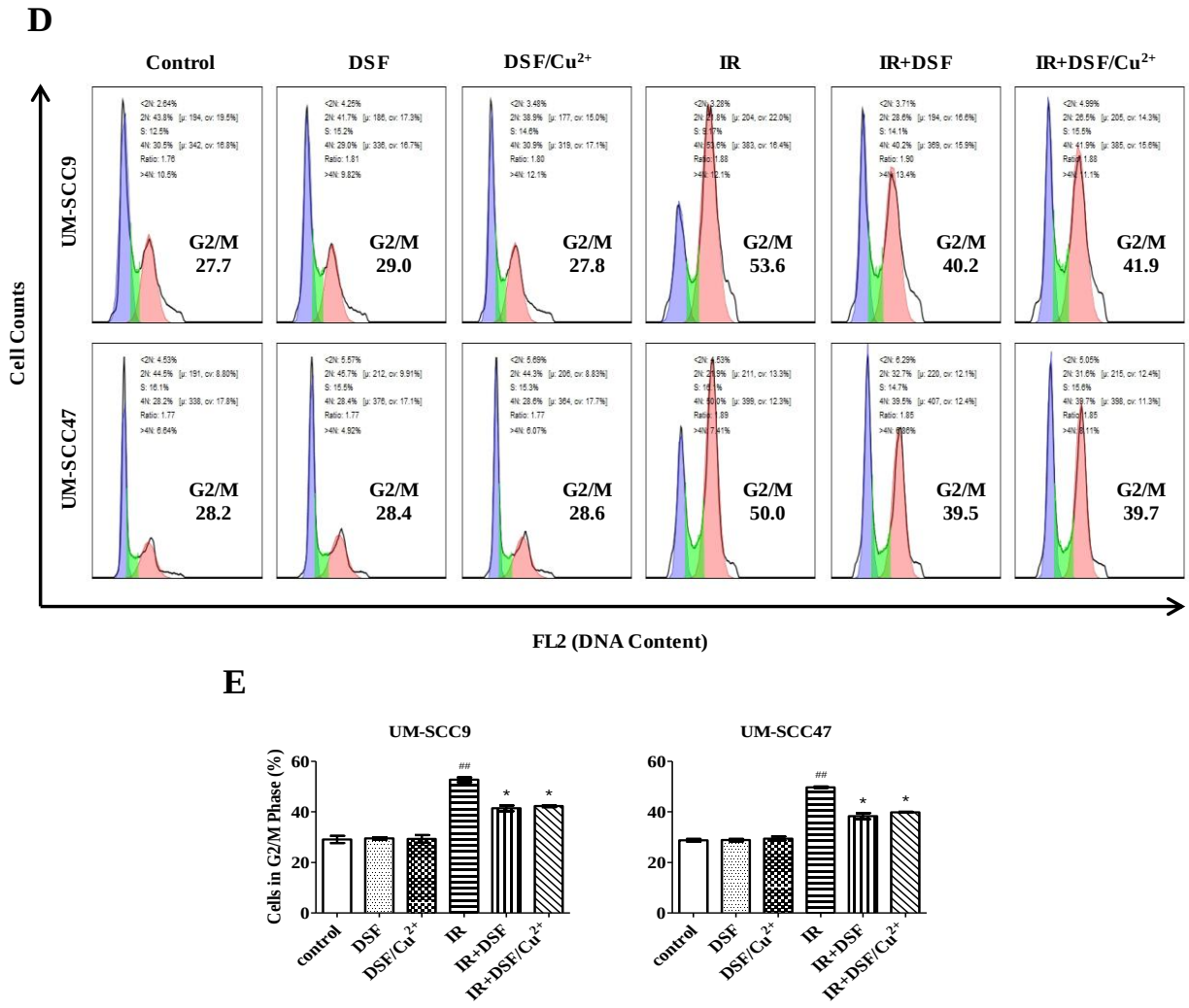

Fig. 10: Radiosensitizing effect of DSF or DSF/Cu^{2+} in HNSCC cell lines.

(A) Cells were pre-treated with various concentrations of DSF or DSF/Cu^{2+} and then irradiated with 10 Gy. After 72 h, viability was analyzed using MTT assay. **(B)** Cells were pre-treated with DSF (1 µM) or DSF/Cu^{2+} (0.1 µM) and then irradiated with 2-6 Gy. After 24 h, cells were reseeded in drug-free medium for 9-12 days. The surviving fraction at different dosages of IR was compared using the LQ-Model formula. **(C)** Cells were treated with the indicated dosages of IR. Cell cycle distributions were detected using flow cytometry 48 h later. The numbers in the graph represent proportions as a percentage of sub-G1 (<2N); G1 (2N); S-phase (S); G2/M phase (4N); and aneuploid cells (>4N). **(D)** Cells were pre-treated with DSF (5 µM) or DSF/Cu^{2+} (0.1 µM) and then irradiated with 10 Gy. 48 h later, the levels of each cell cycle phase were measured using flow cytometry. The numbers in the graph represent proportions as a percentage of sub-G1 (<2N); G1 (2N); S-phase (S); G2/M phase (4N); and aneuploid cells (>4N). **(E)** The percentage of cells in G2/M phase is compared. $^{\#\#}P<0.01$: IR vs. control; $^{*}P<0.05$: IR vs. IR+DSF or IR+DSF/Cu^{2+}; one-way ANOVA.

5.19 Cytotoxic effect by the triple treatment of DSF or DSF/Cu^{2+}, cisplatin and IR in HNSCC cell lines

In previous experiments, we proved that DSF or DSF/Cu^{2+} enhanced the cytotoxic effect of cisplatin and IR by abolishing the G2/M phase arrest in cell cycle. We next investigated the effect of triple exposure on the combination of DSF or DSF/Cu^{2+}, cisplatin, and IR. As shown in Figure 11A and 11B, combining 5 μM DSF or 0.1 μM DSF/Cu^{2+} with 2.5 μM cisplatin increased apoptosis to 34.71% and 26.69% in UM-SCC9, 31% and 25.48% in UM-SCC47, 37.55%, and 31.77% in UM-SCC11B, respectively, which indicated the induction of remarkably higher cell deaths compared to each treatment alone. Furthermore, the combination with IR indicated a significant enhancement of apoptotic cell death. A cytotoxic effect was detected in IR+cisplatin+DSF and IR+cisplatin+DSF/Cu^{2+} with 42.04% and 32.21%in UM-SCC9, 43.9% and 31.91% in UM-SCC47, 45.37% and 38.08% in UM-SCC11B, respectively. Collectively, this effect of suppressing cell growth and inducing apoptosis in triple combination provides a promising clinical treatment strategy to achieve a better chemo-radio-sensitizing effect in HNSCC.

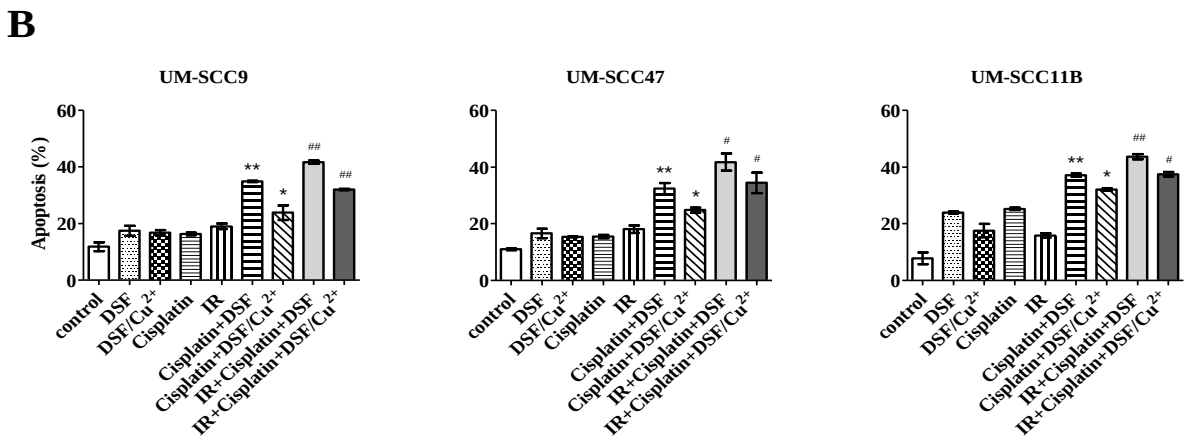

Fig. 11: DSF or DSF/Cu^{2+} combined with cisplatin and IR enhance apoptosis in HNSCC cell lines.

(A) Cells were pre-treated with DSF (5 μM), DSF/Cu^{2+} (0.1 μM), cisplatin (2.5 μM), or a combination of both, then exposed to IR (10 Gy). After 48 h, apoptosis was detected using flow cytometry. **(B)** Graphical representation of the statistical analysis. ***P*<0.01: cisplatin+DSF vs. cisplatin or DSF; **P*<0.05: cisplatin+DSF/Cu^{2+} vs. cisplatin or DSF/Cu^{2+}; $^{\#}P$<0.05 or $^{\#\#}P$<0.01: IR+cisplatin+DSF vs. cisplatin+DSF or IR+cisplatin+DSF/Cu^{2+} vs. cisplatin+DSF/Cu^{2+}, one-way ANOVA.

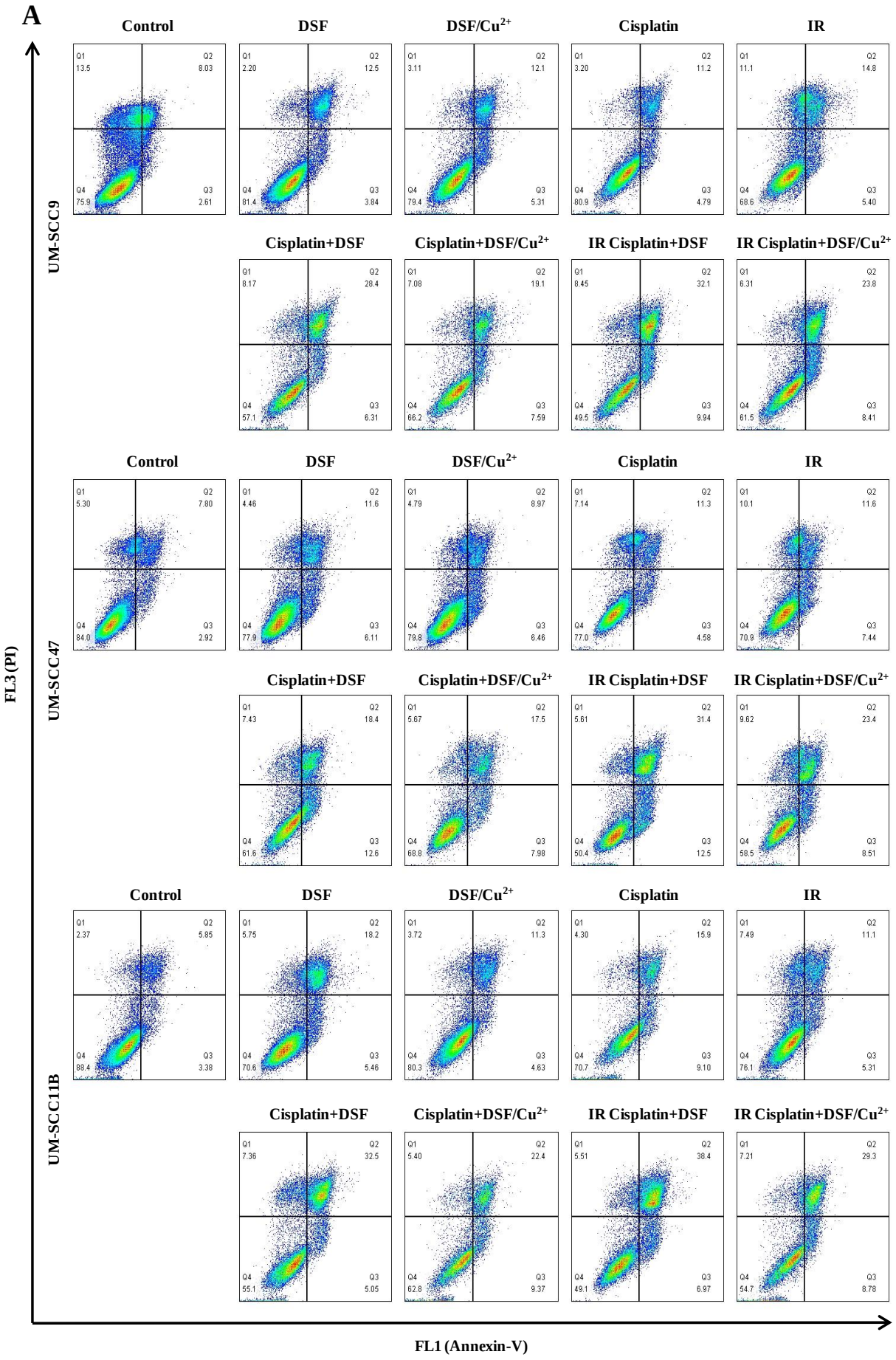
A
Control
DSF
DSF/Cu2+
Cisplatin
IR
Cisplatin+DSF
Cisplatin+DSF/Cu2+
IR Cisplatin+DSF
IR Cisplatin+DSF/Cu2+
UM-SCC9
Q1 13.5
Q2 8.03
Q4 75.9
Q3 2.61
Q1 2.20
Q2 12.5
Q4 81.4
Q3 3.84
Q1 3.11
Q2 12.1
Q4 79.4
Q3 5.31
Q1 3.20
Q2 11.2
Q4 80.9
Q3 4.79
Q1 11.1
Q2 14.8
Q4 68.6
Q3 5.40
Q1 8.17
Q2 28.4
Q4 57.1
Q3 6.31
Q1 7.08
Q2 19.1
Q4 66.2
Q3 7.59
Q1 8.45
Q2 32.1
Q4 49.5
Q3 9.94
Q1 6.31
Q2 23.8
Q4 61.5
Q3 8.41
UM-SCC47
Q1 5.30
Q2 7.80
Q4 84.0
Q3 2.92
Q1 4.46
Q2 11.6
Q4 77.9
Q3 6.11
Q1 4.79
Q2 8.97
Q4 79.8
Q3 6.46
Q1 7.14
Q2 11.3
Q4 77.0
Q3 4.58
Q1 10.1
Q2 11.6
Q4 70.9
Q3 7.44
Q1 7.43
Q2 18.4
Q4 61.6
Q3 12.6
Q1 5.67
Q2 17.5
Q4 68.8
Q3 7.98
Q1 5.61
Q2 31.4
Q4 50.4
Q3 12.5
Q1 9.62
Q2 23.4
Q4 58.5
Q3 8.51
UM-SCC11B
Q1 2.37
Q2 5.85
Q4 88.4
Q3 3.38
Q1 5.75
Q2 18.2
Q4 70.6
Q3 5.46
Q1 3.72
Q2 11.3
Q4 80.3
Q3 4.63
Q1 4.30
Q2 15.9
Q4 70.7
Q3 9.10
Q1 7.49
Q2 11.1
Q4 76.1
Q3 5.31
Q1 7.36
Q2 32.5
Q4 55.1
Q3 5.05
Q1 5.40
Q2 22.4
Q4 62.8
Q3 9.37
Q1 5.51
Q2 38.4
Q4 49.1
Q3 6.97
Q1 7.21
Q2 29.3
Q4 54.7
Q3 8.78
FL3 (PI)
FL1 (Annexin-V)

5.20 Treatment with DSF or DSF/Cu^{2+}, cisplatin, and IR induces ROS generation in HNSCC cell lines

To gain a better understanding of the cytotoxicity in this triple treatment, we explored the generation of ROS after exposure to DSF or DSF/Cu^{2+}, cisplatin and IR. As shown in Figure 12A and 12B, the combination 5 μM DSF with 2.5 μM cisplatin enhanced ROS activity to 38.7% in UM-SCC9, 35.8% in UM-SCC47, 35.9% in UM-SCC11B, respectively, compared to each treatment alone. IR also plays a core role in the accumulation of ROS. When combined with 10 Gy IR, addition of cisplatin and DSF or DSF/Cu^{2+}, further increasing ROS activity was observed with 46.3% and 37.4% in UM-SCC9, 44.0% and 32.5% in UM-SCC47, 46.3% and 34.7% in UM-SCC11B, respectively, compared to unirradiated samples. In conclusion, this evidence proves that the triple treatment of DSF or DSF/Cu^{2+}, cisplatin and IR substantially enhance the ROS generation, which is responsible for the cytotoxic effect and might be emphasized as a potential method in HNSCC treatment.

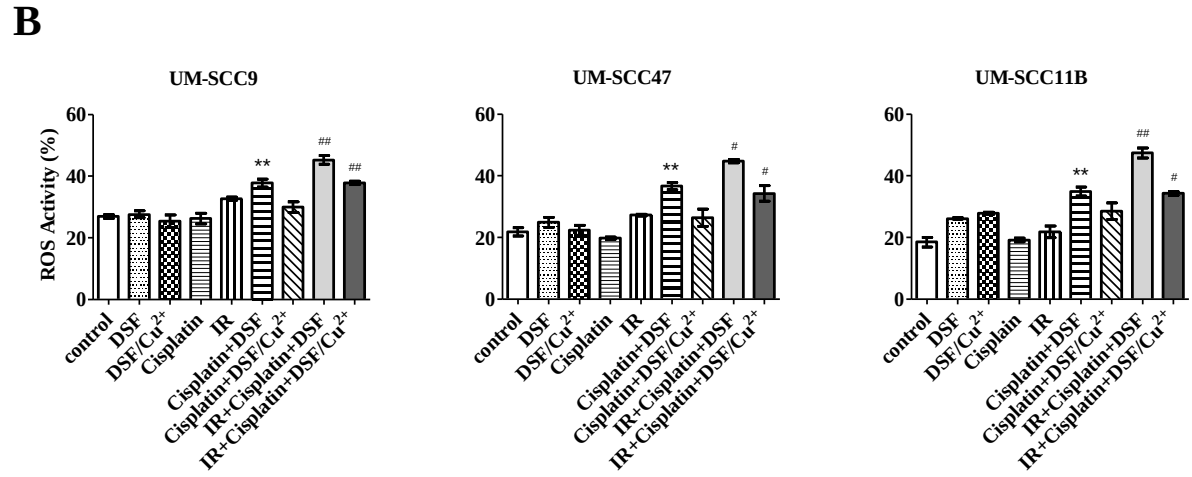

Fig. 12: DSF or DSF/Cu^{2+} combined with cisplatin and IR induce ROS generation in HNSCC cell lines.

(A) Cells were pre-treated with DSF (5 μM), DSF/Cu^{2+} (0.1 μM), cisplatin (2.5 μM), or a combination of both, then exposed to IR (10 Gy). ROS activity was detected 24 h later using flow cytometry. The numbers in the graph represent the ROS activity. **(B)** Graphical representation of the statistical analysis of ROS activity. $^{**}P<0.01$: cisplatin+DSF vs. cisplatin or DSF, $^{\#}P<0.05$ or $^{\#\#}P<0.01$: IR+cisplatin+DSF vs. cisplatin+DSF, or IR+cisplatin+DSF/Cu^{2+} vs. cisplatin+DSF/Cu^{2+}, one-way ANOVA.

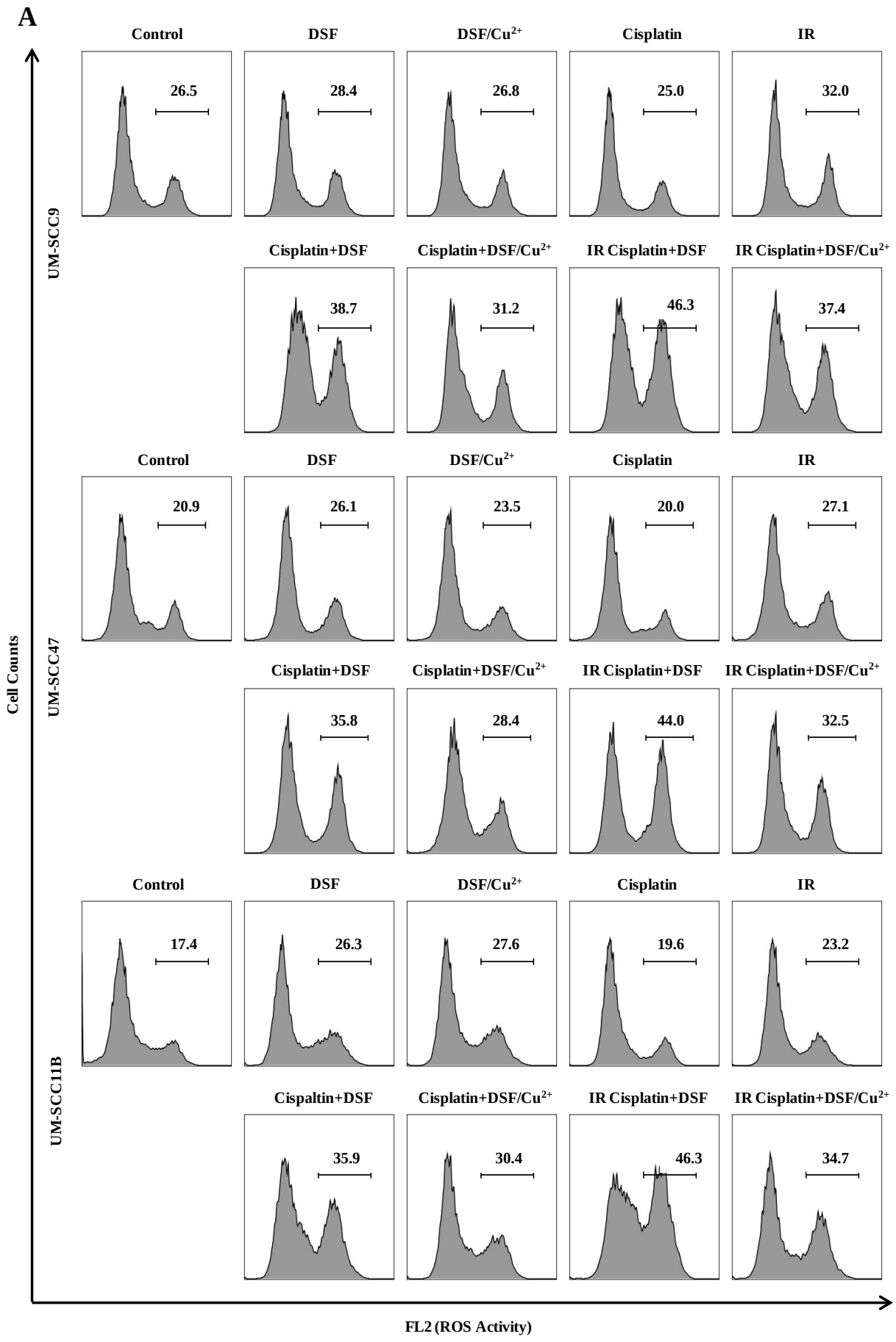
A
Control
DSF
DSF/Cu2+
Cisplatin
IR
26.5
28.4
26.8
25.0
32.0
Cisplatin+DSF
Cisplatin+DSF/Cu2+
IR Cisplatin+DSF
IR Cisplatin+DSF/Cu2+
38.7
31.2
46.3
37.4
UM-SCC9
Control
DSF
DSF/Cu2+
Cisplatin
IR
20.9
26.1
23.5
20.0
27.1
Cisplatin+DSF
Cisplatin+DSF/Cu2+
IR Cisplatin+DSF
IR Cisplatin+DSF/Cu2+
35.8
28.4
44.0
32.5
UM-SCC47
Control
DSF
DSF/Cu2+
Cisplatin
IR
17.4
26.3
27.6
19.6
23.2
Cispaltin+DSF
Cisplatin+DSF/Cu2+
IR Cisplatin+DSF
IR Cisplatin+DSF/Cu2+
35.9
30.4
46.3
34.7
UM-SCC11B
Cell Counts
FL2 (ROS Activity)

6. Discussion

Patients with head and neck cancer encompass a heterogeneous group, and even with advancements in treatment options, the overall survival rate for patients with advanced disease has not changed substantially over recent decades [58]. Therefore, there is a pressing need to improve therapeutic efficacy and develop novel treatment strategies involved in increasing radio-chemotherapy response, counteracting resistance, reducing toxicity and improving clinical outcome. CSCs are identified as a distinct tumor cell population, which play an important role in inherent cancer resistance to conventional treatments, such as CT or RT [59], and in accelerated repopulation and acquired resistance post treatment. They are now being identified and characterized in numbers of solid cancers including HNSCC [60], and highlighting their potential functions and cellular properties is being considered as promising targeted therapy that might enhance treatment response [61]. ALDH activity has been used as a marker to identify and isolate CSCs in a variety of tumors including HNSCC [62]. In recent years, accumulating evidence indicates that ALDH may not only be a surrogate CSC marker but also a functional target for anti-CSC chemo-radio therapy [30, 40].

As an irreversible pan-ALDH inhibitor, DSF is known to inhibit all currently identified cytosolic and mitochondrial ALDH isoforms. This inhibition is probably the basis of its property of sensitizing cells to cytotoxic treatment, and targeting this function might be a novel method for further clinical application, leading to abolish CSCs [63]. DSF and its derivative could form a DSF/Cu^{2+} complex which contributes to transporting Cu into cancer cells, thus overcoming the transporter-controlled regulation of intracellular Cu homoeostasis [40, 46]. Although the serum Cu concentration is elevated in cancer patients, the anticancer activity of DSF is dependent on Cu and many other researchers have demonstrated that Cu supplementation further enhances the antitumor effect of DSF *in vitro* and *in vivo* [64]. Our results show that the viability of HNSCC cells was inhibited by DSF, and the addition of Cu^{2+} further enhanced the cytotoxicity in a dose- and time-dependent manner. These findings were consistent with previous studies, in that DSF has anticancer activity, and cooper potentiates its activity *in vitro* and *in vivo* [65-67].

It is accepted that stem-like cells usually over-express stemness-related markers such as Oct3/4, Sox2, and Nanog, where these genes play essential roles in the regulation of self-renewal and tumorigenicity in the CSC populations of many kinds of tumors [68]. In order to confirm the potential stemness phenotype, SDCs and parallel MDCs from HNSCC cell lines were performed to detect the expression of the CSC-specific markers. A significant up-regulation was detected in

SDCs, and furthermore, SDCs also displayed higher expression of ALDH. In conclusion, these findings proved the presence of a subpopulation of cells with stem-like properties has been identified in SDCs and DSF or DSF/Cu^{2+} complex could inhibit these CSC-features which is relevant for many properties of HNSCC CSCs, such as clonogenicity and spheroid-formation.

Cell migration is defined as the movement of individual cells, cell sheets and clusters from one location to another [69]. The study of cell migration behavior in cancer research is of particular interest, as the main reason of death in cancer patients is related to metastatic progression. Consequently, methods in this investigating this are very useful research strategies for a wide range of disciplines in biomedical sciences, biology, bioengineering, and related fields [70]. Compared to other tools, the *in vitro* scratch assay is particularly suitable for studies on the effects of cell-matrix and cell-cell interactions on cell migration, mimicking cell migration during wound healing *in vivo*, and it is compatible with the imaging of live cells during migration to monitor intracellular events if desired [71]. Collectively, our current observations proved that DSF or DSF/Cu^{2+} could inhibit ALDH activity to abolish the proliferation and self-renewal capacity of CSCs, and to suppress their migratory ability, resulting in the sensitizing of treatment in HNSCC cell lines.

Furthermore, we characterized the ALDH-enriched population using Aldefluor assay followed by FACS sorting, to assess whether they display these CSC-features as well. We showed that ALDH ^{high} cell fractions have increased clonogenic ability, enhanced sphere-formation, lower ROS levels, and more cisplatin resistance compared to ALDH ^{low} cells. These findings indicate that ALDH activity plays an essential role in the drug-resistance and self-renewal capacity of CSCs. Our data has developed in conformity with the results from Raha's group, who detected that the ALDH ^{high} populations share common properties with chemotherapy drug tolerant CSCs. They also suggest that ALDH activity might be one mechanism to protect the CSCs from toxic side effects of therapy and ROS [72]. Specifically, we additionally showed that a therapy-resistant subpopulation of CSCs, with a high expression of ALDH and cisplatin-resistance can preferentially be sensitized by DSF, which could be a chemo-sensitizer in HNSCC cell lines.

Even though the therapeutic efficacy of DSF or DSF/Cu^{2+} was investigated *in vivo* and *in vitro*, complete remission was not achieved by mono treatment. To improve this therapeutic effect, drug combination might be considered, delivering a small molecular agent, DSF, to the tumor tissue to suppress CSCs, and standard anti-cancer reagent to target the bulk tumor cells. While cisplatin is currently one of the most common chemotherapeutic agents used in the treatment, its

success and efficacy wane because of therapeutic resistance. Our study showed a synergistic effect of DSF in the combination with cisplatin resulting in CI<1, and this associated with reduced cellular proliferation and enhanced cisplatin-induced cytotoxicity.

Cancer cells show a deregulated cell cycle progression, with either overexpression of positive regulators, or inhibition of negative regulators, which provide them with unrestrained replication potential [73]. Deregulation of the cell cycle has been implicated in most human cancers and leads to cell proliferation, chromosome instability, and loss of genomic integrity [74]. The cytotoxicity of cisplatin is mediated by its interaction with DNA, resulting in the formation of DNA adducts which activate several signal transduction pathways and culminate in the activation of apoptosis [75]. IR induces various DNA-damage, but double-strand breaks are the most cytotoxic effects, which can perturb cell cycle progression at different stages, mainly inducing G2/M phase arrest [76]. This arrest provides time to repair DNA damage and to prevent mitotic catastrophes and apoptosis [77]. Many studies have shown that abrogation of the G2 checkpoint can potentiate cell death induced by IR [78] or DNA-damaging agents [79], which supports the G2 checkpoint as a potential therapeutic target that may sensitize cells to chemo- and radio-therapy.

We showed that the cell cycle was paused at the G2/M phase when cells were exposed to cisplatin, and additional treatment by DSF or DSF/Cu^{2+} could abolish this block leading to DNA damage, which is a mechanism for cell death. Moreover, after treatment with IR, the G2/M cell fractions were increased in a dose-dependent manner, which suggest elevated checkpoint activation in HNSCC cell lines in response to DNA damage. We next demonstrated that DSF or DSF/Cu^{2+} potentiated the efficacy of IR through abolishing the G2/M arrest, and then have the ability to inhibit IR-induced G2 checkpoint activation, which could lead more damaged cells to enter mitosis without appropriate repair, leading to cell death and thereby significantly enhancing the cytotoxic effect of IR. This hypothesis may contribute to an underlying mechanism for the radio-sensitization caused by DSF or DSF/Cu^{2+} in HNSCC cell lines. Furthermore, DSF or DSF/Cu^{2+} strongly inhibited HNSCC clonogenicity to such an effect that few colonies could be isolated, resulting in a linear response being shown with increasing dosage, and a curve established with this combination therapy.

In comparison with normal tissues, cancer cells generally possess high ROS activity and can tolerate higher levels of ROS [80]. Our findings demonstrated that DSF or DSF/Cu^{2+} alone, or in a combination with cisplatin and IR, lead to a remarkable intracellular ROS burst, which may

result in the effect of reduced scavenging and less detoxification, and develop to be a novel method for treatment of CSC subpopulations and ultimately cancers. DSF or DSF/Cu^{2+} reduced the ROS tolerance by inhibiting ALDH and targeting CSCs in HNSCC cell lines.

In addition, a number of clinical trials have been established to identify the promising anti-cancer activity of DSF. Phase II clinical trials were performed to investigate DSF in newly diagnosed glioblastoma multiform (NCT 01777919), and to measure the combination effect with cisplatin in metastatic non-small cell lung cancer (NCT 00312819). Other phase I trials in hormone refractory cancers with liver (NCT 00742911) and melanoma metastases (NCT 00256230), and prostate cancer (NCT 01118741), are still ongoing.

Even though the impressive tolerance of DSF and its powerful anti-cancer capacity have been researched for years, very few successful cases had been reported in clinic [81]. The possible reason for this discrepancy might be that the pharmacokinetics and pharmacodynamics of DSF appear to highly variable among subjects. Surprisingly, clinical studies on the kinetics of DSF have shown that a single-dose administration of 250 mg DSF leads to a maximum serum concentration of approximately 1.3μM and can reach 1.4μM after repeated doses [82]. Consequently, the enrichment and metabolism of DSF in the liver become the bottleneck for its translation into the clinic therapy. The Nano-encapsulated DSF, such as liposomal- and poly lactic-co-glycolic acid (PLGA), were used to prevent these eliminations. The nano-precipitation method protects the thiol groups in DSF, extends its half-life in the blood from less than 2 min to over 7 h, and successfully delivers the intact DSF into tumor tissues [83, 84]. This modification of DSF would be a beneficial approach for its delivery and improve its stability during the process of position targeting.

However, due to the time-consuming and high-cost procedures in the development of new therapeutic drugs, the rate of new approvals are still very low. Therefore, drug repurposing or drug repositioning, utilizing the previously unknown anti-cancer effects of “old” drugs, can be a promising strategy to identify prospective new therapeutic uses [85]. DSF has been used as an anti-alcoholism drug for over 60 years with acceptable pre-clinical and clinical acceptable side effects, and it could therefore be a valuable approach to repurpose it into a promising new anti-cancer drug, or an adjuvant treatment for sensitization in combination with other therapies.

In this study, we determined DSF or DSF/Cu^{2+} was cytotoxic by itself in a dose- and time-dependent manner, and investigated the effect of ROS generation, which might be the potential

underlying mechanism responsible for its anti-cancer activity in HNSCC cell lines. Moreover, we demonstrated significant inhibition of the expression in CSC markers, including Oct3/4, Sox2, and Nanog, decreasing the growth of CSCs as well as reducing their cellular self-renewal capacity. Of even greater interest, our comparative analysis assessed the inhibitory effect of DSF or DSF/Cu^{2+} on ALDH expression and migration ability, which may have also proved the systems for eliminating CSC-features. The combined DSF and cisplatin created a synergistic cytotoxicity in HNSCC cell lines, and DSF sensitized the cancer cells - especially the ALDH ^{high} cells - effectively for cisplatin treatment, and reversed its resistance. Furthermore, we also demonstrated that DSF or DSF/Cu^{2+} could sensitize the effectiveness of IR and cisplatin treatment, which were associated with suppressing the survival fraction, abolishing the G2/M phase arrest in the cell cycle, improving the apoptotic rate and inducing ROS generation as well. Taken together, these observations indicated that DSF or DSF/Cu^{2+} could target CSCs and lead to stemness-related inhibition, which resulted in intrinsically cytotoxic, and chemo-radio-sensitizing effects. Overall, our present work suggests that DSF has potentially important implications for future therapeutic approaches in head and neck cancers.

7. Reference

1. Ghantous, Y. and I. Abu Elnaaj, [Global Incidence and Risk Factors of Oral Cancer]. Harefuah, 2017. 156(10): p. 645-649.

2. Howlader, N., A. Noone, M. Krapcho, D. Miller, K. Bishop, C. Kosary, M. Yu, J. Ruhl, Z. Tatalovich, and A. Mariotto, SEER cancer statistics review, 1975–2014. Bethesda, MD: National Cancer Institute, 2017. 2018.

3. Le, X. and E.Y. Hanna, Optimal regimen of cisplatin in squamous cell carcinoma of head and neck yet to be determined. Ann Transl Med, 2018. 6(11): p. 229.

4. Lassen, P., J.G. Eriksen, A. Krogdahl, M.H. Therkildsen, B.P. Ulhoi, M. Overgaard, L. Specht, E. Andersen, J. Johansen, L.J. Andersen, C. Grau, J. Overgaard, H. Danish, and G. Neck Cancer, The influence of HPV-associated p16-expression on accelerated fractionated radiotherapy in head and neck cancer: evaluation of the randomised DAHANCA 6&7 trial. Radiother Oncol, 2011. 100(1): p. 49-55.

5. Poole, M.E., S.L. Sailer, J.G. Rosenman, J.E. Tepper, M.C. Weissler, W.W. Shockley, W.G. Yarbrough, H.C. Pillsbury, 3rd, M.J. Schell, and S.A. Bernard, Chemoradiation for locally advanced squamous cell carcinoma of the head and neck for organ preservation and palliation. Arch Otolaryngol Head Neck Surg, 2001. 127(12): p. 1446-50.

6. Kim, J.S., J.H. Lee, W.W. Jeong, D.H. Choi, H.J. Cha, D.H. Kim, J.K. Kwon, S.E. Park, J.H. Park, H.R. Cho, S.H. Lee, S.K. Park, B.J. Lee, Y.J. Min, and J.W. Park, Reactive oxygen species-dependent EndoG release mediates cisplatin-induced caspase-independent apoptosis in human head and neck squamous carcinoma cells. Int J Cancer, 2008. 122(3): p. 672-80.

7. Deavall, D.G., E.A. Martin, J.M. Horner, and R. Roberts, Drug-induced oxidative stress and toxicity. J Toxicol, 2012. 2012: p. 645460.

8. Song, W., Z. Tang, N. Shen, H. Yu, Y. Jia, D. Zhang, J. Jiang, C. He, H. Tian, and X. Chen, Combining disulfiram and poly(l-glutamic acid)-cisplatin conjugates for combating cisplatin resistance. J Control Release, 2016. 231: p. 94-102.

9. Barr, M.P., S.G. Gray, A.C. Hoffmann, R.A. Hilger, J. Thomale, J.D. O'Flaherty, D.A. Fennell, D. Richard, J.J. O'Leary, and K.J. O'Byrne, Generation and characterisation of cisplatin-resistant non-small cell lung cancer cell lines displaying a stem-like signature. PLoS One, 2013. 8(1): p. e54193.

10. Pignon, J.P., A. le Maitre, E. Maillard, J. Bourhis, and M.-N.C. Group, Meta-analysis of chemotherapy in head and neck cancer (MACH-NC): an update on 93 randomised trials and 17,346 patients. Radiother Oncol, 2009. 92(1): p. 4-14.

11. Tejpal, G., A. Jaiprakash, B. Susovan, S. Ghosh-Laskar, V. Murthy, and A. Budrukkar, IMRT and IGRT in head and neck cancer: Have we delivered what we promised? Indian J Surg Oncol, 2010. 1(2): p. 166-85.

12. Nias, A., An introduction to radiobiology. 1998: John Wiley & Sons.

13. Eriksson, D., P.-O. Löfroth, L. Johansson, K.Å. Riklund, and T. Stigbrand, Cell cycle disturbances and mitotic catastrophes in HeLa Hep2 cells following 2.5 to 10 Gy of ionizing radiation. Clinical Cancer Research, 2007. 13(18): p. 5501s-5508s.

14. Zhou, B.-B.S. and S.J. Elledge, The DNA damage response: putting checkpoints in perspective. Nature, 2000. 408(6811): p. 433.

15. Chen, Z., Z. Xiao, W.z. Gu, J. Xue, M.H. Bui, P. Kovar, G. Li, G. Wang, Z.F. Tao, and Y. Tong, Selective Chk1 inhibitors differentially sensitize p53-deficient cancer cells to cancer therapeutics. International journal of cancer, 2006. 119(12): p. 2784-2794.

16. Lacombe, J., D. Azria, A. Mange, and J. Solassol, Proteomic approaches to identify biomarkers predictive of radiotherapy outcomes. Expert Rev Proteomics, 2013.

10(1): p. 33-42.

17. Ahmed, K.M. and J.J. Li, ATM-NF-kappaB connection as a target for tumor radiosensitization. Curr Cancer Drug Targets, 2007. 7(4): p. 335-42.

18. de Jong, M.C., J. Jelle, R. Grénman, L.F. Wessels, R. Kerkhoven, H. te Riele, M.W. van den Brekel, M. Verheij, and A.C. Begg, Pretreatment microRNA expression impacting on epithelial-to-mesenchymal transition predicts intrinsic radiosensitivity in head and neck cancer cell lines and patients. Clinical Cancer Research, 2015. 21(24): p. 5630-5638.

19. O'Brien, C.A., A. Kreso, and J.E. Dick, Cancer stem cells in solid tumors: an overview. Semin Radiat Oncol, 2009. 19(2): p. 71-7.

20. Han, D., G. Wu, C. Chang, F. Zhu, Y. Xiao, Q. Li, T. Zhang, and L. Zhang, Disulfiram inhibits TGF-β-induced epithelial-mesenchymal transition and stem-like features in breast cancer via ERK/NF-κB/Snail pathway. Oncotarget, 2015. 6(38): p. 40907.

21. Kulsum, S., H.V. Sudheendra, R. Pandian, D.R. Ravindra, G. Siddappa, P. Chevour, B. Ramachandran, M. Sagar, A. Jayaprakash, and A. Mehta, Cancer stem cell mediated acquired chemoresistance in head and neck cancer can be abrogated by aldehyde dehydrogenase 1 A1 inhibition. Molecular carcinogenesis, 2017. 56(2): p. 694-711.

22. Zhang, Y., Z. Wang, J. Yu, J. Shi, C. Wang, W. Fu, Z. Chen, and J. Yang, Cancer stem-like cells contribute to cisplatin resistance and progression in bladder cancer. Cancer Lett, 2012. 322(1): p. 70-7.

23. Chang, C.C., G.S. Shieh, P. Wu, C.C. Lin, A.L. Shiau, and C.L. Wu, Oct-3/4 expression reflects tumor progression and regulates motility of bladder cancer cells. Cancer Res, 2008. 68(15): p. 6281-91.

24. Chiou, S.H., M.L. Wang, Y.T. Chou, C.J. Chen, C.F. Hong, W.J. Hsieh, H.T. Chang, Y.S. Chen, T.W. Lin, H.S. Hsu, and C.W. Wu, Coexpression of Oct4 and Nanog enhances malignancy in lung adenocarcinoma by inducing cancer stem cell-like properties and epithelial-mesenchymal transdifferentiation. Cancer Res, 2010. 70(24): p. 10433-44.

25. Ezeh, U.I., P.J. Turek, R.A. Reijo, and A.T. Clark, Human embryonic stem cell genes OCT4, NANOG, STELLAR, and GDF3 are expressed in both seminoma and breast carcinoma. Cancer, 2005. 104(10): p. 2255-65.

26. Wen, J., J.Y. Park, K.H. Park, H.W. Chung, S. Bang, S.W. Park, and S.Y. Song, Oct4 and Nanog expression is associated with early stages of pancreatic carcinogenesis. Pancreas, 2010. 39(5): p. 622-6.

27. Pan, Y., J. Jiao, C. Zhou, Q. Cheng, Y. Hu, and H. Chen, Nanog is highly expressed in ovarian serous cystadenocarcinoma and correlated with clinical stage and pathological grade. Pathobiology, 2010. 77(6): p. 283-8.

28. Harper, L.J., D.E. Costea, L. Gammon, B. Fazil, A. Biddle, and I.C. Mackenzie, Normal and malignant epithelial cells with stem-like properties have an extended G2 cell cycle phase that is associated with apoptotic resistance. BMC cancer, 2010. 10(1): p. 166.

29. Tomita, H., K. Tanaka, T. Tanaka, and A. Hara, Aldehyde dehydrogenase 1A1 in stem cells and cancer. Oncotarget, 2016. 7(10): p. 11018.

30. Bertrand, G., M. Maalouf, A. Boivin, P. Battiston-Montagne, M. Beuve, A. Levy, P. Jalade, C. Fournier, D. Ardail, N. Magne, G. Alphonse, and C. Rodriguez-Lafrasse, Targeting head and neck cancer stem cells to overcome resistance to photon and carbon ion radiation. Stem Cell Rev, 2014. 10(1): p. 114-26.

31. Prince, M.E., L. Zhou, J.S. Moyer, H. Tao, L. Lu, J. Owen, M. Egenti, F. Zheng, A.E. Chang, and J. Xia, Evaluation of the immunogenicity of ALDHhigh human head

and neck squamous cell carcinoma cancer stem cells in vitro. Oral oncology, 2016. 59: p. 30-42.

32. Yang, L., Y. Ren, X. Yu, F. Qian, H.-l. Xiao, W.-g. Wang, S.-l. Xu, J. Yang, W. Cui, and Q. Liu, ALDH1A1 defines invasive cancer stem-like cells and predicts poor prognosis in patients with esophageal squamous cell carcinoma. Modern Pathology, 2014. 27(5): p. 775.

33. Zhang, G., L. Ma, Y.-K. Xie, X.-B. Miao, and C. Jin, Esophageal cancer tumorspheres involve cancer stem-like populations with elevated aldehyde dehydrogenase enzymatic activity. Molecular medicine reports, 2012. 6(3): p. 519-524.

34. Zhang, X., R. Komaki, L. Wang, B. Fang, and J.Y. Chang, Treatment of radioresistant stem-like esophageal cancer cells by an apoptotic gene-armed, telomerase-specific oncolytic adenovirus. Clinical Cancer Research, 2008. 14(9): p. 2813-2823.

35. Yu, J., A. Alharbi, H. Shan, Y. Hao, B. Snetsinger, M.J. Rauh, and X. Yang, TAZ induces lung cancer stem cell properties and tumorigenesis by up-regulating ALDH1A1. Oncotarget, 2017. 8(24): p. 38426.

36. Fasehee, H., R. Dinarvand, A. Ghavamzadeh, M. Esfandyari-Manesh, H. Moradian, S. Faghihi, and S.H. Ghaffari, Delivery of disulfiram into breast cancer cells using folate-receptor-targeted PLGA-PEG nanoparticles: in vitro and in vivo investigations. J Nanobiotechnology, 2016. 14: p. 32.

37. Yoshida, A., L.C. Hsu, and V. Dave, Retinal oxidation activity and biological role of human cytosolic aldehyde dehydrogenase. Enzyme, 1992. 46(4-5): p. 239-44.

38. Wang, W., H.L. McLeod, and J. Cassidy, Disulfiram-mediated inhibition of NF-κB activity enhances cytotoxicity of 5-fluorouracil in human colorectal cancer cell lines. International journal of cancer, 2003. 104(4): p. 504-511.

39. Zhang, H., D. Chen, J. Ringler, W. Chen, Q.C. Cui, S.P. Ethier, Q.P. Dou, and G. Wu, Disulfiram treatment facilitates phosphoinositide 3-kinase inhibition in human breast cancer cells in vitro and in vivo. Cancer Res, 2010. 70(10): p. 3996-4004.

40. Liu, P., S. Brown, T. Goktug, P. Channathodiyil, V. Kannappan, J.P. Hugnot, P.O. Guichet, X. Bian, A.L. Armesilla, J.L. Darling, and W. Wang, Cytotoxic effect of disulfiram/copper on human glioblastoma cell lines and ALDH-positive cancer-stem-like cells. Br J Cancer, 2012. 107(9): p. 1488-97.

41. Lin, J., M.C. Haffner, Y. Zhang, B.H. Lee, W.N. Brennen, J. Britton, S.K. Kachhap, J.S. Shim, J.O. Liu, and W.G. Nelson, Disulfiram is a DNA demethylating agent and inhibits prostate cancer cell growth. The Prostate, 2011. 71(4): p. 333-343.

42. Morrison, B.W., N.A. Doudican, K.R. Patel, and S.J. Orlow, Disulfiram induces copper-dependent stimulation of reactive oxygen species and activation of the extrinsic apoptotic pathway in melanoma. Melanoma Res, 2010. 20(1): p. 11-20.

43. Rae, C., M. Tesson, J.W. Babich, M. Boyd, A. Sorensen, and R.J. Mairs, The role of copper in disulfiram-induced toxicity and radiosensitization of cancer cells. J Nucl Med, 2013. 54(6): p. 953-60.

44. Ma, I. and A.L. Allan, The role of human aldehyde dehydrogenase in normal and cancer stem cells. Stem Cell Rev, 2011. 7(2): p. 292-306.

45. Qian, X., X. Nie, W. Yao, K. Klinghammer, H. Sudhoff, A.M. Kaufmann, and A.E. Albers, Reactive oxygen species in cancer stem cells of head and neck squamous cancer. Semin Cancer Biol, 2018.

46. Cen, D., D. Brayton, B. Shahandeh, F.L. Meyskens, Jr., and P.J. Farmer, Disulfiram facilitates intracellular Cu uptake and induces apoptosis in human melanoma cells. J Med Chem, 2004. 47(27): p. 6914-20.

47. Wang, Y., W. Li, S.S. Patel, J. Cong, N. Zhang, F. Sabbatino, X. Liu, Y. Qi, P. Huang, H. Lee, A. Taghian, J.J. Li, A.B. DeLeo, S. Ferrone, M.W. Epperly, C.R. Ferrone,

A. Ly, E.F. Brachtel, and X. Wang, Blocking the formation of radiation-induced breast cancer stem cells. Oncotarget, 2014. 5(11): p. 3743-55.

48. Lewis, D.J., P. Deshmukh, A.A. Tedstone, F. Tuna, and P. O'Brien, On the interaction of copper(II) with disulfiram. Chem Commun (Camb), 2014. 50(87): p. 13334-7.

49. Vanchieri, C., Cutting copper curbs angiogenesis, studies show. J Natl Cancer Inst, 2000. 92(15): p. 1202-3.

50. Brewer, G.J., Anticopper therapy against cancer and diseases of inflammation and fibrosis. Drug Discov Today, 2005. 10(16): p. 1103-9.

51. Garofalo, J.A., E. Erlandson, E.W. Strong, M. Lesser, F. Gerold, R. Spiro, M. Schwartz, and R.A. Good, Serum zinc, serum copper, and the Cu/Zn ratio in patients with epidermoid cancers of the head and neck. J Surg Oncol, 1980. 15(4): p. 381-6.

52. Calderon-Aparicio, A., M. Strasberg-Rieber, and M. Rieber, Disulfiram anti-cancer efficacy without copper overload is enhanced by extracellular H2O2 generation: antagonism by tetrathiomolybdate. Oncotarget, 2015. 6(30): p. 29771-81.

53. Tesson, M., G. Anselmi, C. Bell, and R. Mairs, Cell cycle specific radiosensitisation by the disulfiram and copper complex. Oncotarget, 2017. 8(39): p. 65900-65916.

54. Zhang, N., J.N. Fu, and T.C. Chou, Synergistic combination of microtubule targeting anticancer fludelone with cytoprotective panaxytriol derived from panax ginseng against MX-1 cells in vitro: experimental design and data analysis using the combination index method. Am J Cancer Res, 2016. 6(1): p. 97-104.

55. Kramer, N., A. Walzl, C. Unger, M. Rosner, G. Krupitza, M. Hengstschlager, and H. Dolznig, In vitro cell migration and invasion assays. Mutat Res, 2013. 752(1): p. 10-24.

56. Park, Y.M., S.Y. Lee, S.W. Park, and S.H. Kim, Role of cancer stem cell in radioresistant head and neck cancer. Auris Nasus Larynx, 2016. 43(5): p. 556-61.

57. Eccles, S.A., C. Box, and W. Court, Cell migration/invasion assays and their application in cancer drug discovery. Biotechnol Annu Rev, 2005. 11: p. 391-421.

58. Leemans, C.R., B.J. Braakhuis, and R.H. Brakenhoff, The molecular biology of head and neck cancer. Nat Rev Cancer, 2011. 11(1): p. 9-22.

59. Cojoc, M., K. Mabert, M.H. Muders, and A. Dubrovska, A role for cancer stem cells in therapy resistance: cellular and molecular mechanisms. Semin Cancer Biol, 2015. 31: p. 16-27.

60. Bhaijee, F., D.J. Pepper, K.T. Pitman, and D. Bell, Cancer stem cells in head and neck squamous cell carcinoma: a review of current knowledge and future applications. Head Neck, 2012. 34(6): p. 894-9.

61. Lynam-Lennon, N., S. Heavey, G. Sommerville, B.A. Bibby, B. Ffrench, J. Quinn, C. Gasch, J.J. O'Leary, M.F. Gallagher, J.V. Reynolds, and S.G. Maher, MicroRNA-17 is downregulated in esophageal adenocarcinoma cancer stem-like cells and promotes a radioresistant phenotype. Oncotarget, 2017. 8(7): p. 11400-11413.

62. Chen, Y.C., Y.W. Chen, H.S. Hsu, L.M. Tseng, P.I. Huang, K.H. Lu, D.T. Chen, L.K. Tai, M.C. Yung, S.C. Chang, H.H. Ku, S.H. Chiou, and W.L. Lo, Aldehyde dehydrogenase 1 is a putative marker for cancer stem cells in head and neck squamous cancer. Biochem Biophys Res Commun, 2009. 385(3): p. 307-13.

63. Kulsum, S., H.V. Sudheendra, R. Pandian, D.R. Ravindra, G. Siddappa, N. R, P. Chevour, B. Ramachandran, M. Sagar, A. Jayaprakash, A. Mehta, V. Kekatpure, N. Hedne, M.A. Kuriakose, and A. Suresh, Cancer stem cell mediated acquired chemoresistance in head and neck cancer can be abrogated by aldehyde dehydrogenase 1 A1 inhibition. Mol Carcinog, 2017. 56(2): p. 694-711.

64. Xu, B., P. Shi, I.S. Fombon, Y. Zhang, F. Huang, W. Wang, and S. Zhou, Disulfiram/copper complex activated JNK/c-jun pathway and sensitized cytotoxicity of doxorubicin in doxorubicin resistant leukemia HL60 cells. Blood Cells Mol Dis, 2011. 47(4): p. 264-9.

65. Chen, D., Q.C. Cui, H. Yang, and Q.P. Dou, Disulfiram, a clinically used anti-alcoholism drug and copper-binding agent, induces apoptotic cell death in breast cancer cultures and xenografts via inhibition of the proteasome activity. Cancer Res, 2006. 66(21): p. 10425-33.

66. Liu, X., L. Wang, W. Cui, X. Yuan, L. Lin, Q. Cao, N. Wang, Y. Li, W. Guo, X. Zhang, C. Wu, and J. Yang, Targeting ALDH1A1 by disulfiram/copper complex inhibits non-small cell lung cancer recurrence driven by ALDH-positive cancer stem cells. Oncotarget, 2016. 7(36): p. 58516-58530.

67. Li, Y., S.Y. Fu, L.H. Wang, F.Y. Wang, N.N. Wang, Q. Cao, Y.T. Wang, J.Y. Yang, and C.F. Wu, Copper improves the anti-angiogenic activity of disulfiram through the EGFR/Src/VEGF pathway in gliomas. Cancer Lett, 2015. 369(1): p. 86-96.

68. MacDonagh, L., M.F. Gallagher, B. Ffrench, C. Gasch, E. Breen, S.G. Gray, S. Nicholson, N. Leonard, R. Ryan, V. Young, J.J. O'Leary, S. Cuffe, S.P. Finn, K.J. O'Byrne, and M.P. Barr, Targeting the cancer stem cell marker, aldehyde dehydrogenase 1, to circumvent cisplatin resistance in NSCLC. Oncotarget, 2017. 8(42): p. 72544-72563.

69. Friedl, P. and K. Wolf, Tumour-cell invasion and migration: diversity and escape mechanisms. Nat Rev Cancer, 2003. 3(5): p. 362-74.

70. Justus, C.R., N. Leffler, M. Ruiz-Echevarria, and L.V. Yang, In vitro cell migration and invasion assays. J Vis Exp, 2014(88).

71. Liang, C.C., A.Y. Park, and J.L. Guan, In vitro scratch assay: a convenient and inexpensive method for analysis of cell migration in vitro. Nat Protoc, 2007. 2(2): p. 329-33.

72. Raha, D., T.R. Wilson, J. Peng, D. Peterson, P. Yue, M. Evangelista, C. Wilson, M. Merchant, and J. Settleman, The cancer stem cell marker aldehyde dehydrogenase is required to maintain a drug-tolerant tumor cell subpopulation. Cancer Res, 2014. 74(13): p. 3579-90.

73. Deep, G. and R. Agarwal, New combination therapies with cell-cycle agents. Curr Opin Investig Drugs, 2008. 9(6): p. 591-604.

74. Ansari, S.S., A.K. Sharma, M. Zepp, E. Ivanova, F. Bergmann, R. König, and M.R. Berger, Upregulation of cell cycle genes in head and neck cancer patients may be antagonized by erufosine's down regulation of cell cycle processes in OSCC cells. Oncotarget, 2018. 9(5): p. 5797.

75. Kelland, L.R., Preclinical perspectives on platinum resistance. Drugs, 2000. 59 Suppl 4: p. 1-8; discussion 37-8.

76. Tenzer, A. and M. Pruschy, Potentiation of DNA-damage-induced cytotoxicity by G2checkpoint abrogators. Current Medicinal Chemistry-Anti-Cancer Agents, 2003. 3(1): p. 35-46.

77. Kim, Y.M., I.H. Jeong, and H. Pyo, Celecoxib enhances the radiosensitizing effect of 7-hydroxystaurosporine (UCN-01) in human lung cancer cell lines. Int J Radiat Oncol Biol Phys, 2012. 83(3): p. e399-407.

78. Syljuasen, R.G., C.S. Sorensen, J. Nylandsted, C. Lukas, J. Lukas, and J. Bartek, Inhibition of Chk1 by CEP-3891 accelerates mitotic nuclear fragmentation in response to ionizing Radiation. Cancer Res, 2004. 64(24): p. 9035-40.

79. Chen, Z., Z. Xiao, W.Z. Gu, J. Xue, M.H. Bui, P. Kovar, G. Li, G. Wang, Z.F. Tao, Y. Tong, N.H. Lin, H.L. Sham, J.Y. Wang, T.J. Sowin, S.H. Rosenberg, and H. Zhang, Selective Chk1 inhibitors differentially sensitize p53-deficient cancer cells to

cancer therapeutics. Int J Cancer, 2006. 119(12): p. 2784-94.

80. Fruehauf, J.P. and F.L. Meyskens, Jr., Reactive oxygen species: a breath of life or death? Clin Cancer Res, 2007. 13(3): p. 789-94.

81. Askgaard, G., S. Friis, J. Hallas, L.C. Thygesen, and A. Pottegård, Use of disulfiram and risk of cancer: a population-based case–control study. European Journal of Cancer Prevention, 2014. 23(3): p. 225-232.

82. Faiman, M.D., J.C. Jensen, and R.B. Lacoursiere, Elimination kinetics of disulfiram in alcoholics after single and repeated doses. Clinical Pharmacology & Therapeutics, 1984. 36(4): p. 520-526.

83. Wang, Z., J. Tan, C. McConville, V. Kannappan, P.E. Tawari, J. Brown, J. Ding, A.L. Armesilla, J.M. Irache, and Q.-B. Mei, Poly lactic-co-glycolic acid controlled delivery of disulfiram to target liver cancer stem-like cells. Nanomedicine: Nanotechnology, Biology and Medicine, 2017. 13(2): p. 641-657.

84. Butcher, K., V. Kannappan, R.S. Kilari, M.R. Morris, C. McConville, A.L. Armesilla, and W. Wang, Investigation of the key chemical structures involved in the anticancer activity of disulfiram in A549 non-small cell lung cancer cell line. BMC cancer, 2018. 18(1): p. 753.

85. Park, Y.M., Y.Y. Go, S.H. Shin, J.G. Cho, J.S. Woo, and J.J. Song, Anti-cancer effects of disulfiram in head and neck squamous cell carcinoma via autophagic cell death. PLoS One, 2018. 13(9): p. e0203069.

8. Curriculum Vitae

My curriculum vitae does not appear in the electronic version of my paper for reasons of data protection.

9. Affidavit

I, Wenhao Yao, certify under penalty of perjury by my own signature that I have submitted the thesis on the topic “Disulfiram (Antabuse) acts as a potent chemo-radio-sensitizer and abolishes stem cells in HNSCC cell lines *in vitro*”. I wrote this thesis independently and without assistance from third parties, I used no other aids than the listed sources and resources.

All points based literally or in spirit on publications or presentations of other authors are, as such, in proper citations (see "uniform requirements for manuscripts (URM)" the ICMJE www.icmje.org) indicated. The sections on methodology (in particular practical work, laboratory requirements, statistical processing) and results (in particular images, graphics and tables) correspond to the URM (s.o) and are answered by me. My interests in any publications to this dissertation correspond to those that are specified in the following joint declaration with the responsible person and supervisor. All publications resulting from this thesis and which I am author correspond to the URM (see above) and I am solely responsible.

The importance of this affidavit and the criminal consequences of a false affidavit (section 156,161 of the Criminal Code) are known to me and I understand the rights and responsibilities stated therein.

Date Signature

10. Acknowledgements

How time flies. I still remember the first time I stood in front of the building in the Campus Benjamin Franklin, and I told myself, that will be a new exciting journey. Now, four years later, and at this moment, I am still on the trip to purse my dream.

Here, I would like to give my special gratitude to my supervisor Dr. Andreas Albers, who offering the valuable chance for me to study in the Charité-Universitätsmedizin Berlin. His ideas and comments are the bright lamps for me especially when the experiments in the trouble. Even though he is busy about the clinic works, he still takes the time to discuss the project with me, and tries his best to solve all the problems.

Great thankful for Dr. Andreas M. Kaufmann, who always gives me a hand whenever I am in the trouble, and provides me with the professional ideas and suggestions. His support and guidance are the appreciated during my whole life along.

During my work here, I usually closely and successfully collaborated with all the members in our group. Thanks to Dana Schiller, who arrange all the facilities in the lab for everyone to make all the things go well Thanks to Jinfeng Xu for giving the advices to my experiments. Thanks to Sarina Sarina and Lili Liang who help me a lot in the daily life. Thanks to Sarah Thies, Anna Sophie Skof, Aleksandra Pesic and all others. I have much appreciation for all your friendship and I will never forget the happy time together with you.

I own my great gratitude to my parents, who always support me whatever happens and for your love and encouragement, I can finally stand here. You are my spiritual pillar to make my whole life full of sunshine.